Final Report

Program and KPI:	V.RDP.2018
Report Title:	MEXA Assisted Offal Sortation Technical Feasibility (a technical report from ALMTech for MLA)
Prepared by:	Ed Morton Rapiscan Systems
Date published:	22th October 2021

This project is supported by funding from the Australian Government Department of Agriculture, Water and the Environment as part of its Rural R&D for Profit programme in partnership with Research & Development Corporations, Commercial Companies, State Departments & Universities.

This project is supported by funding from the Australian Government Department of Agriculture, Water and the Environment as part of its Rural R&D for Profit programme in partnership with Research & Development Corporations, Commercial Companies, State Departments & Universities.

Acknowledgements

This project is supported by funding from the Australian Government Department of Agriculture, Water and the Environment as part of its Rural R&D for Profit programme in partnership with Research & Development Corporations, Commercial Companies, State Departments & Universities.

Abstract

This program seeks to determine whether a multi-sensor platform combining multi-energy X-ray (MEXA) with visible and shortwave infra-red (SWIR) hyperspectral camera data can detect defects in organs and viscera to assess animal health.

The program is a collaboration between MLA, Rapiscan Systems and the University of Sydney. A multi-sensor platform, software and algorithms were developed as a proof-of-concept to detect defects in organs and other viscera. The University of Sydney, through its animal and veterinary science team at the Camden Campus, was responsible for the scientific work associated with organ selection for study, reporting on anatomy and pathology and analysing how multi-sensor technology can aid in automated offal inspection at the abattoir scale. The platform was able to differentiate organs by species and type with up to 92% accuracy, and organs with defects with up to 96% accuracy, 91% sensitivity, 100% specificity. The platform seems promising for the automatic detection of defects in sheep offal but larger datasets are required to validate and improve algorithms. Work in beef cattle has not been done in depth and this is an area proposed for further research.

This project is supported by funding from the Australian Government Department of Agriculture, Water and the Environment as part of its Rural R&D for Profit programme in partnership with Research & Development Corporations, Commercial Companies, State Departments & Universities.

Executive Summary

This program forms part of V.RDP.2000, advanced measurement technologies for globally competitive Australian meat value chains. In this specific project, V.RDP.2018 MEXA assisted offal sortation technical feasibility, a team comprising MLA, Rapiscan Systems and the University of Sydney is exploring the use of a multi-sensor imaging platform comprising dual-view multi-energy X-ray imaging (MEXA), visible waveband hyperspectral camera imaging and short wave infra-red (SWIR) hyperspectral camera imaging. The MEXA technology was developed under MDC program P.PSH.0886 while the hyperspectral camera sensor was developed under a precursor to the current program, V.RDP.2016.

In the present work, V.RDP.2018, the MEXA and hyperspectral imaging sensors have been combined into a single system that has been installed at the University of Sydney, Camden Campus. The unit is now in continuous operation by the University of Sydney team including Rapiscan's sponsored PhD student, Cassius Coombs. A series of samples have been acquired from abattoirs, these have been scanned by the multi-sensor system. Automatic identification of defects in sheep organs has shown to be possible using hyperspectral imaging with up 92% accuracy. The dataset from beef organs was small to do any sensible analysis and this is one of the areas proposed for future work. In addition, future work should use larger datasets to validate and strengthen the algorithms. The algorithms could also be improved using shape analysis in addition to spectral information, and using both the spectral data with the X-ray data.

This project is supported by funding from the Australian Government Department of Agriculture, Water and the Environment as part of its Rural R&D for Profit programme in partnership with Research & Development Corporations, Commercial Companies, State Departments & Universities.

Contents

This project is supported by funding from the Australian Government Department of Agriculture, Water and the Environment as part of its Rural R&D for Profit programme in partnership with Research & Development Corporations, Commercial Companies, State Departments & Universities.

1 Introduction

At the end of the prior V.RDP.2016 program, Rapiscan Systems had just received two hyperspectral cameras, one for the visible wavelength range (400nm to 900nm) and one for the short wave infra-red (SWIR) wavelength range (900nm to 1800nm). It had also completed the build of its dual-view multi-energy X-ray (MEXA) scanner. The scanner and camera systems were bought together by Rapiscan's team in Melbourne, VIC. This work was completed around March 2020.

The V.RDP.2018 program was started in March 2020 with a six-month program duration. During the first two months of the program, Rapiscan's team conducted software development and system calibration work to prepare the system for installation at the University of Sydney. The necessary radiation protection work was completed to allow the scanner to be operated in the University laboratories. The multi-sensor scanner was delivered to the University laboratory and commissioned for use in May 2020.

During May and June, further improvements were made to the system software to facilitate the scanning process and in July 2020 and considerable number of scans were conducted. The analysis work on this data is now starting but remains an open work in progress.

2 Methodology

2.1 Scanner Development and Installation

The 6040DV-ME MEXA scanner comprises a dual-view X-ray scanner with one vertical up-shooter view and one side-shooter view. It is fitted with high spatial resolution multi-energy photon counting X-ray sensors. It has been upgraded at the Rapiscan Systems Melbourne facility to add visible and short-wave infra-red (SWIR) hyperspectral camera sensors.

2.1.1 System Integration at Rapiscan Systems, Melbourne

2.1.1.1 Sample Illumination

To achieve good quality image data from the hyperspectral camera systems, it is necessary to provide sufficient illumination at all wavelengths in the (otherwise dark) imaging region. A variety of imaging light sources were evaluated including white LED's, halogen lamps and a QIR heating lamp as commonly found in food counters to keep food warm.

To evaluate emission wavelength from each light source, a white reflective card was placed in the X-ray scanning tunnel to reflect light from the illumination sources back to the line-scan geometry hyperspectral imaging cameras. The results of these measurements are shown in Figure 1 for the visible wavelength camera and in Figure 2 for the SWIR camera.

In the SWIR region, the QIR sensor was almost an order of magnitude brighter than the halogen lamp while there was no illumination in this region from the LED. Therefore, the QIR sensor was adopted for the broadband illumination task.

This project is supported by funding from the Australian Government Department of Agriculture, Water and the Environment as part of its Rural R&D for Profit programme in partnership with Research & Development Corporations, Commercial Companies, State Departments & Universities.

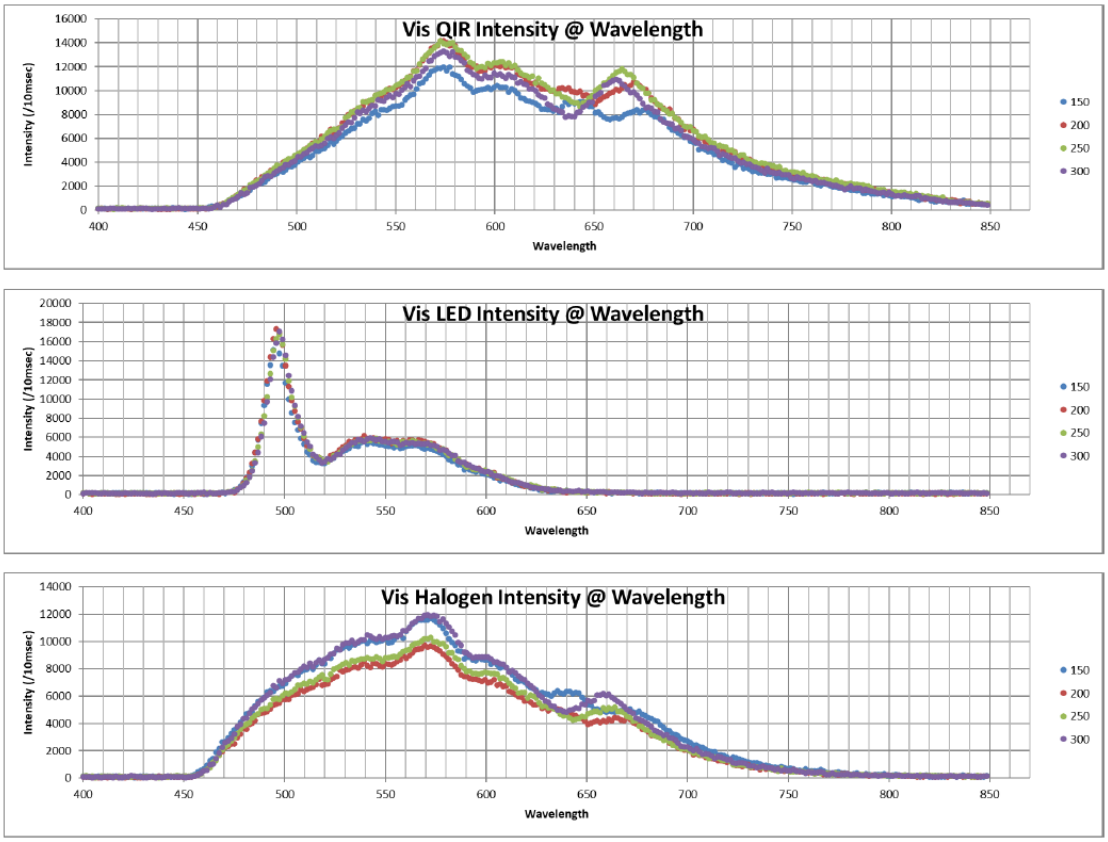

Figure 1: Selection of illumination source for visible camera wavelengths as a function of scan rate (Hz).

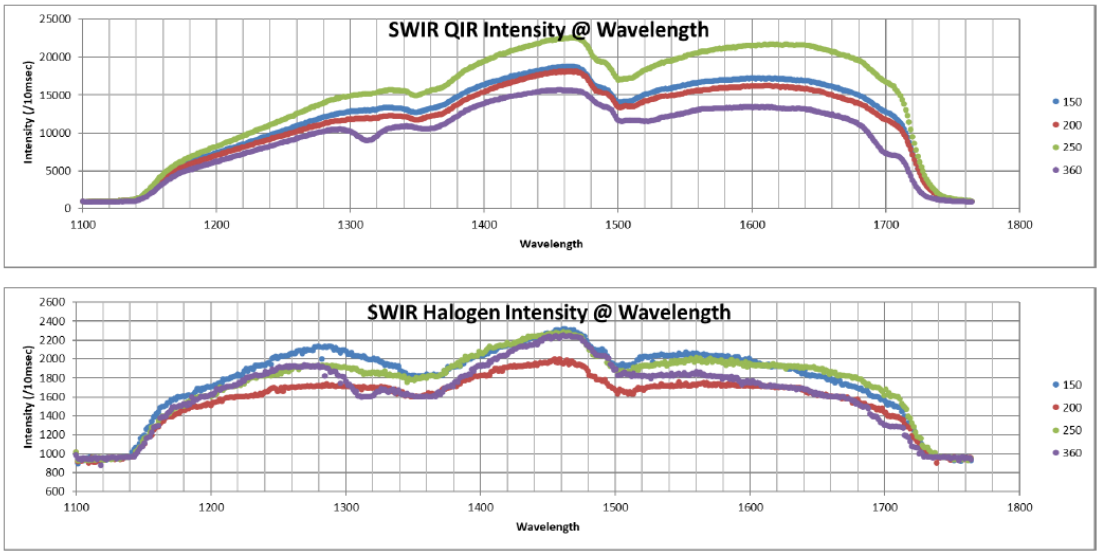

Figure 2: Selection of illumination source for short wave infra-red (SWIR) wavelengths as a function of scan rate (Hz).

Given that the QIR sensor is very efficient at producing heat, a modification to the X-ray scanner control system was made such that the QIR light source is only switched on when the X-ray beam is on. This restricts heating in the scanning tunnel to only those seconds when a scan is actually being conducted.

This project is supported by funding from the Australian Government Department of Agriculture, Water and the Environment as part of its Rural R&D for Profit programme in partnership with Research & Development Corporations, Commercial Companies, State Departments & Universities.

2.1.1.2 Simultaneous Capture

A series of tests were then conducted using both X-ray absorbing and optically reflective bar code patterns to verify that the correct X-ray data is associated with the correct visible light data and that these are both associated with the correct SWIR data. Figure 3 shows an example bar code scanned simultaneously using X-ray, visible and SWIR sensors. Alignment between the various sensors is reasonable.

Figure 3: Image alignment of X-ray data (left), visible data (centre) and SWIR data (right).

2.1.1.3 X-ray Scanning and Calibration

Figure 4 and Figure 5 show MEXA X-ray image data for both the central vertical up-shooter view (Figure 4) and for the side-shooter view (Figure 5). To the left of both views is a standard X-ray test piece used in the aviation industry for image quality performance validation. To the right of both views are X-ray images of beef offal packed and purchased from a local wholesale butcher.

Figure 4: Multi-energy X-ray image data – central up-shooter view. Left: X-ray image quality test piece. Right: Beef offal.

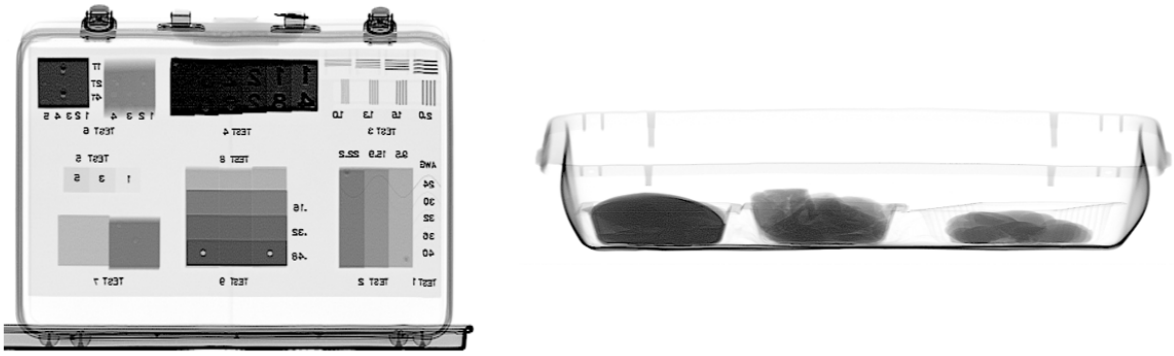

This project is supported by funding from the Australian Government Department of Agriculture, Water and the Environment as part of its Rural R&D for Profit programme in partnership with Research & Development Corporations, Commercial Companies, State Departments & Universities.

Figure 5: Multi-energy X-ray image data – side-shooter view. Left: X-ray image quality test piece. Right: Beef offal.

At the time that these images were taken, the final energy calibration of the energy thresholds of each multi-energy channel had not been completed and this is the origin of the vertical streaks in the X-ray image data. Solving this calibration problem is the current focus of the Rapiscan Systems physics and sensor team and it is planned that the multi-sensor system at the University of Sydney will be upgraded shortly with the improved calibration procedure. This is expected to eliminate the vertical streak artefacts and provide the qualitative data necessary to calculate effective atomic number along each line integral from source to detector.

2.1.1.4 Preliminary Offal Characterisation

While still at the Rapiscan Systems facility in Melbourne, some lamb pluck (heart, liver and lungs) was acquired from a local butcher and X-ray image data was acquired as shown in Figure 6. The sample was first imaged while still fresh and then it was imaged again after some days of decay.

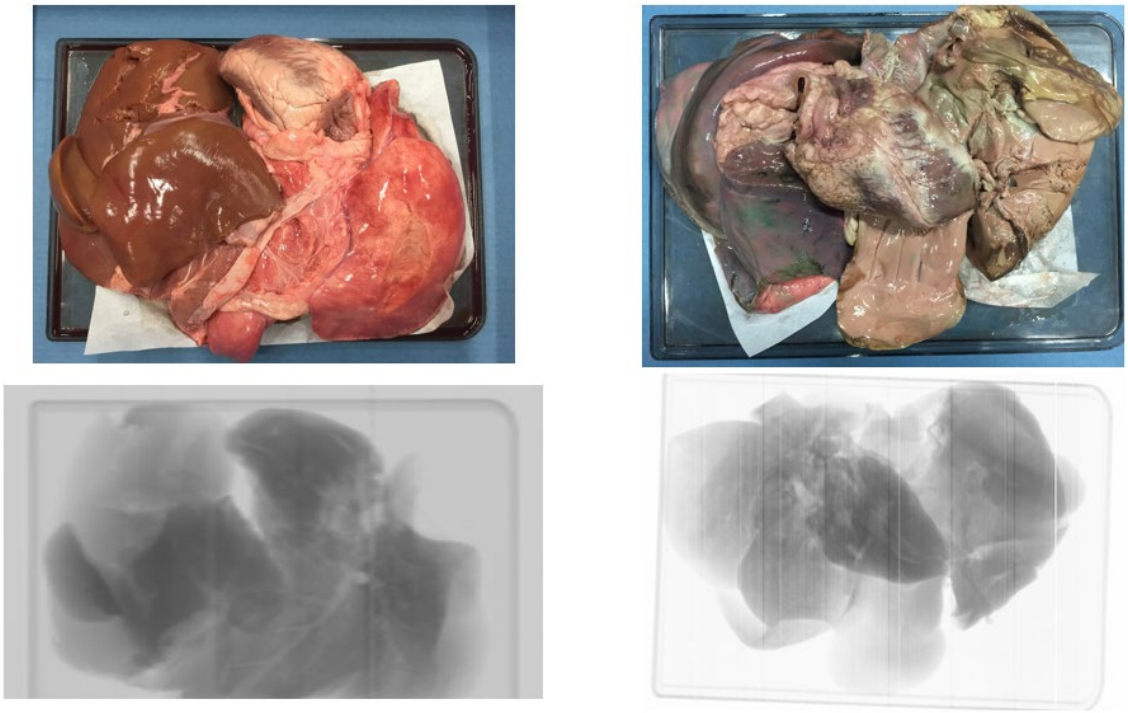

Figure 6: Photograph and corresponding MEXA images for fresh and ripe lamb pluck.

In these images, the heart is quite clearly identifiable in the X-ray data as distinct to the liver and lungs. There is good scope for using an automated algorithm for identification of the heart in these images. It is likely that to unscramble lung from liver will require a combination of vertical and horizontal view X-ray data in order to determine the thickness of this tissue and so calculate density and effective atomic number at each location in the image with a reasonable level of accuracy. We believe the loss of image contrast over time is in some part a consequence of blood leaching from the organs. This work is in the backlog for the Rapiscan Systems algorithm team.

2.1.1.5 Optimising Capture Performance

As part of the imaging optimisation work, it was necessary to find settings for the X-ray, optical and SWIR hyperspectral cameras to provide the most useful diagnostic image data within the overall

This project is supported by funding from the Australian Government Department of Agriculture, Water and the Environment as part of its Rural R&D for Profit programme in partnership with Research & Development Corporations, Commercial Companies, State Departments & Universities.

operating constraints of each device. Following an extensive experimental program, the optimal operating conditions selected for the multi-sensor system were determined. The results are shown in Figure 7.

Modality	Frequency / Frames per sec	Image / Field of View	Exposure
ME xray	300Hz	1232 pixels, full tunnel	3.3msec
Visible	150FPS	300 x 430, ¾ tunnel	6.4msec
SWIR	150FPS	512 x 256, ½ tunnel	3.5msec

Figure 7: Offal screening system final optimisation settings.

With these optimised settings, the synchronised image data for the MEXA, visible and SWIR sensors is shown in Figure 8. The MEXA data covers the entire field of view. The visible hyperspectral data covers 75% of the field of view while the SWIR hyperspectral data covers 50% of the field of view. The restricted field of view for the two hyperspectral cameras is due to bandwidth constraints in the Gigabit Ethernet camera interface to the host PC.

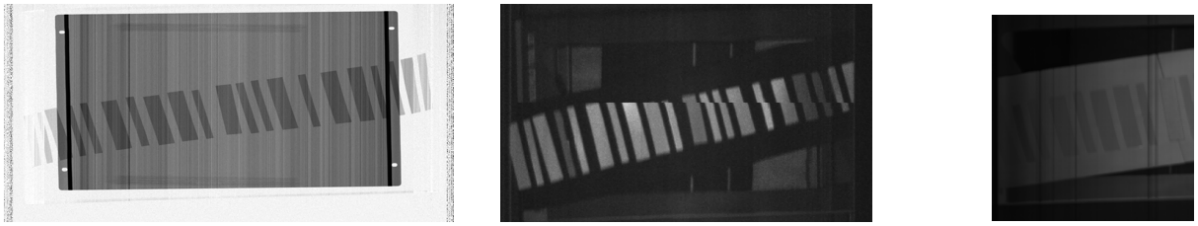

Figure 8: Image synchronisation for the optimised offal screening system. Left: X-ray, Centre: Visible, Right: Short Wave Infra-Red (SWIR).

Rapiscan Systems is in communication with the camera manufacturer about reducing spectral resolution in order to reduce camera output data rate and so allow full field of view imaging. Should this camera upgrade become available, it will be fitted to the University of Sydney system.

2.1.2 Scanner Installation at University of Sydney

The multi-sensor system was shipped from Melbourne and installed at the University of Sydney Camden Campus on 20th May 2020. The self-contained scanning system is not abattoir compatible and so currently needs to be used with samples in sealed trays to avoid the requirement for washdown.

Figure 9 shows the system immediately after installation. Samples are loaded from the left, pass through the scanner and emerge from the right-hand side of the equipment.

Figure 10 shows the complete installation in the laboratory at the University of Sydney.

This project is supported by funding from the Australian Government Department of Agriculture, Water and the Environment as part of its Rural R&D for Profit programme in partnership with Research & Development Corporations, Commercial Companies, State Departments & Universities.

Figure 11 shows the in-feed conveyor and operator workstation.

Figure 9: Photograph of the multi-sensor system once installed at the University of Sydney.

Figure 10: View of the installed system with the side-shooter X-ray view just visible to the left of the main system enclosure.

This project is supported by funding from the Australian Government Department of Agriculture, Water and the Environment as part of its Rural R&D for Profit programme in partnership with Research & Development Corporations, Commercial Companies, State Departments & Universities.

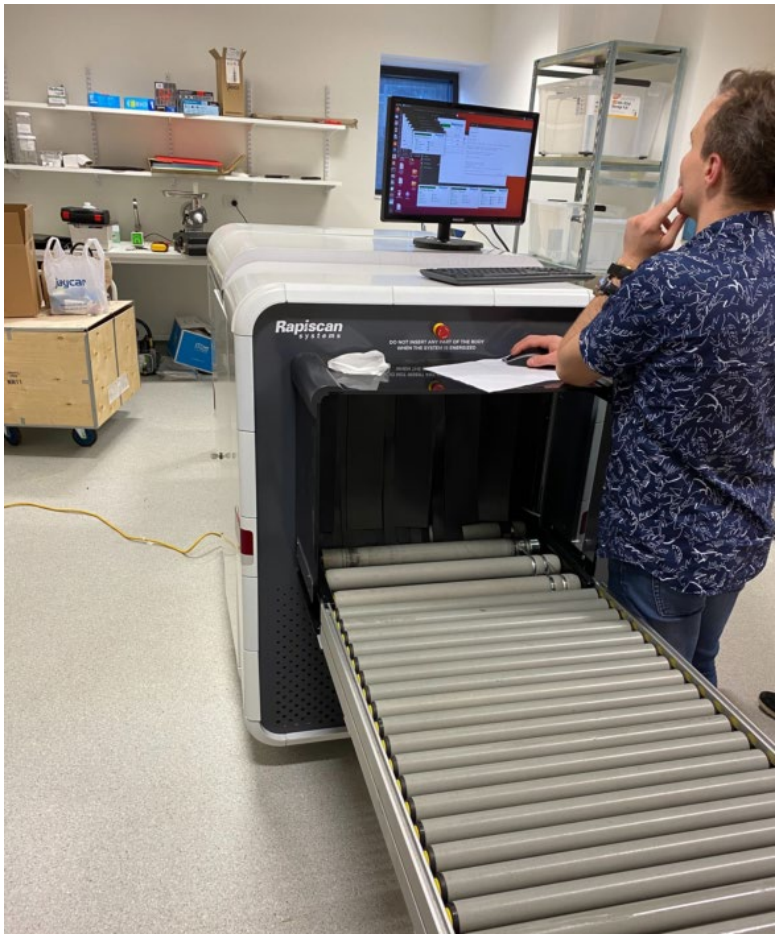

Figure 11: Photograph of the installed multi-sensor system showing the passive roller bed onto which samples are placed in trays prior to X-ray scanning.

Since installation in May 2020, the Rapiscan team have made a number of site visits to Camden related to software integration improvements. This work is on-going, but the system continues to head towards full stability as a reliable scientific data collections platform. The key areas of work underway are:

1. Real-time energy and intensity calibration of the MEXA sensor arrays
2. Finalising system integration of the two hyperspectral cameras at close to full GigE bandwidth on both cameras
3. Providing synchronised store to disk and recall for MEXA, visible and SWIR camera data in DICOM format with associated TDR's etc.
4. Providing a consolidated user interface for detailed review of all image types simultaneously

2.2 Veterinary Science

Under the operating licence for the University or Sydney laboratory where the equipment is installed, all biological materials not passed for human consumption must be wrapped to prevent spread of contaminants. This means that the items to be inspected must be covered in a plastic or metal enclosure.

This project is supported by funding from the Australian Government Department of Agriculture, Water and the Environment as part of its Rural R&D for Profit programme in partnership with Research & Development Corporations, Commercial Companies, State Departments & Universities.

In order to achieve hyperspectral sensing of samples in the visible and SWIR wavelength regions, the enclosure must be transparent over the top surface of the sample. Further, the cover should be non-reflective as far as possible to prevent direct reflection of the light source back into the camera sensor.

The most appropriate solution is to use a thin plastic layer over the samples (e.g. cling-film) and a key activity of the veterinary science program has been to establish a means for wrapping samples and handing them in a way which provides good sensor data and that meets the operating licence for the laboratory.

The team has also acquired and selected a variety of offal and other samples for analysis and has conducted trial scans to assess system configuration, stability and data accuracy prior to conducting detailed clinical studies since these will require stable system operation over extended periods with good data calibration etc.

2.3 Algorithm Development

At this stage, the sensing platform and data collection process is still going through some optimisation to achieve reliable and consistent imaging data. Once the system has become stable, the algorithm development process will start in earnest.

3 Results

3.1 Hyperspectral Imaging Performance

3.1.1 Image Alignment

In order to verify data acquisition synchronisation between the two hyperspectral cameras, a simulation pattern was developed for playback from each camera. In this case, one camera outputted magenta data and the other green data. When perfectly aligned, the result will sum to white and will otherwise result in magenta or green leading or trailing pixels.

The result of this pattern for a badly synchronised hyperspectral imaging system is shown in Figure 12. Here, several green and magenta regions are seen. In a perfectly synchronised system all test bars appear in white colour. The system now operates in synchronised fashion for all scans and the test bars are uniform white colour.

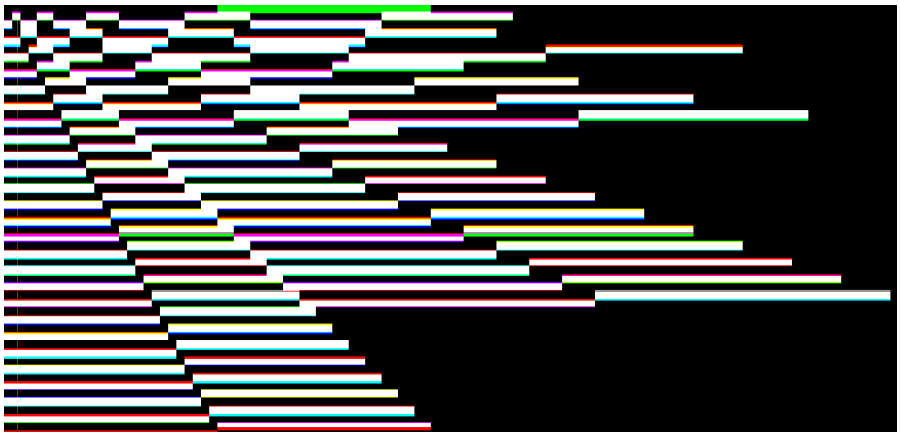

This project is supported by funding from the Australian Government Department of Agriculture, Water and the Environment as part of its Rural R&D for Profit programme in partnership with Research & Development Corporations, Commercial Companies, State Departments & Universities.

Figure 12: Test pattern for checking synchronisation of the hyperspectral camera systems.

3.1.1 Image Viewing

Hyperspectral image data for liver from a lamb is shown in Figure 13. To the left is data from the visible hyperspectral imaging camera, coloured with a pseudo colour scale (from blue to red). To the right is data from the SWIR hyperspectral camera. There is strong contrast between the fat region at the centre of the image and the lung tissue region at the periphery of the image.

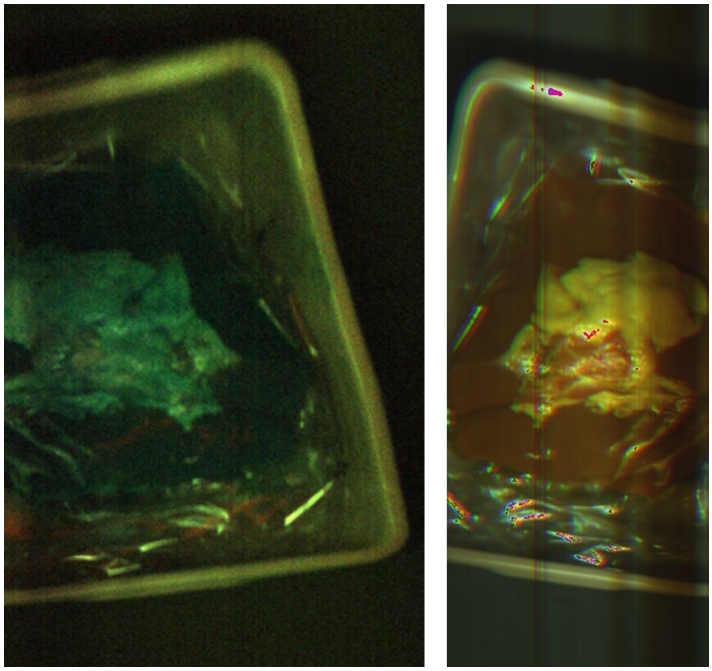

Figure 13: Camera Images of lamb liver. Visible image (left) and hyperspectral image (right). Both images are shown in pseudo colour.

3.2 Veterinary Science

3.2.1 Offal Image Program

The samples that have been scanned to date are listed in Figure 14. In the period to end June, the system was unstable and not able to provide good quality X-ray or hyperspectral image data.

- Preliminary meat and offal (20 May) healthy organs (heart, liver, kidney)
- 2 livers with fluke worms (24 June) – hyperspectral not working, x-ray was poor
- 18 frozen newborn dead lambs (24 June) – hyperspectral not working, x-ray was poor
- 18 thawed newborn dead lambs (1 July) – hyperspectral not working, x-ray was poor
- 1 liver with fluke (3 July)
- 20 pieces of carcass trim with caseous lymphadenitis (cheesy gland), 12 condemned and 12 clean organs (9 July)
- 13 dead lambs (14 July)
- 4 selected lungs with pneumonia from dead lambs (15 July)

Figure 14: Summary of scan data taken for veterinary study since installation of the scanner.

This project is supported by funding from the Australian Government Department of Agriculture, Water and the Environment as part of its Rural R&D for Profit programme in partnership with Research & Development Corporations, Commercial Companies, State Departments & Universities.

The software team continue to work on many aspects of the system design to ensure reliable data. Effective July 2020, system reliability has improved to the point where routine data collection can occur with repeatable results.

3.2.2 Beef Liver Fluke

A first clinical study was conducted of a Wagyu beef liver containing fluke worm (*Fasciola hepatica*). Photographs of the liver following partial dissection are shown in Figure 15. Associated X-ray image data is shown in Figure 16.

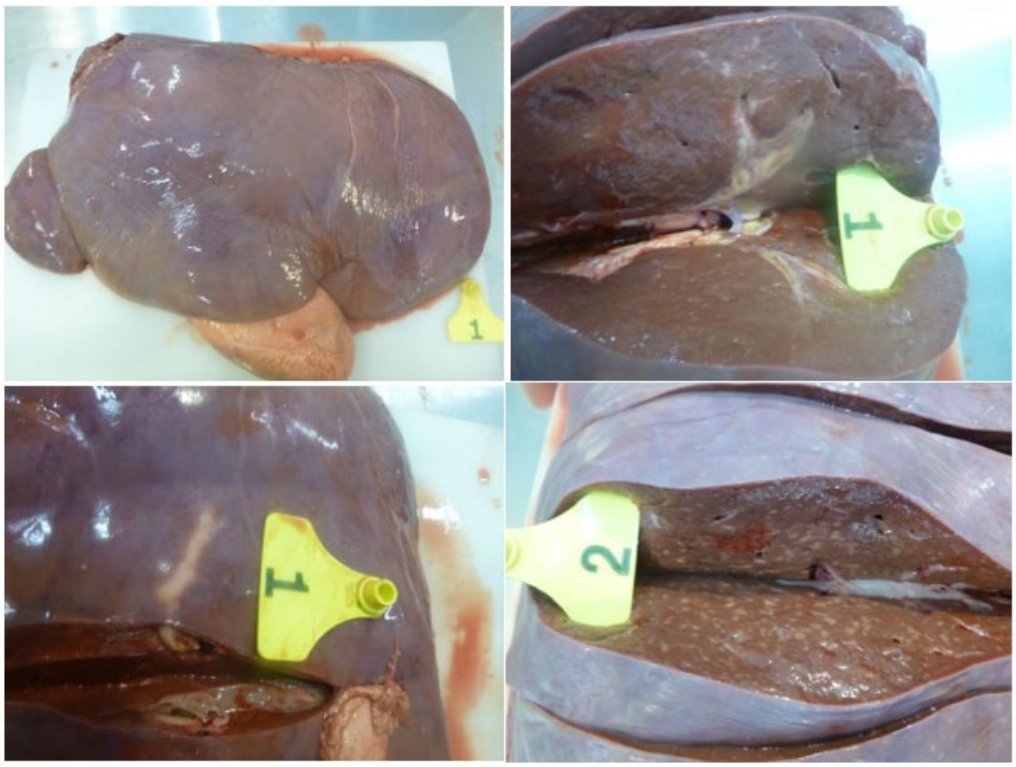

Figure 15: Cattle liver with fluke worm for which X-ray scan data was acquired.

This project is supported by funding from the Australian Government Department of Agriculture, Water and the Environment as part of its Rural R&D for Profit programme in partnership with Research & Development Corporations, Commercial Companies, State Departments & Universities.

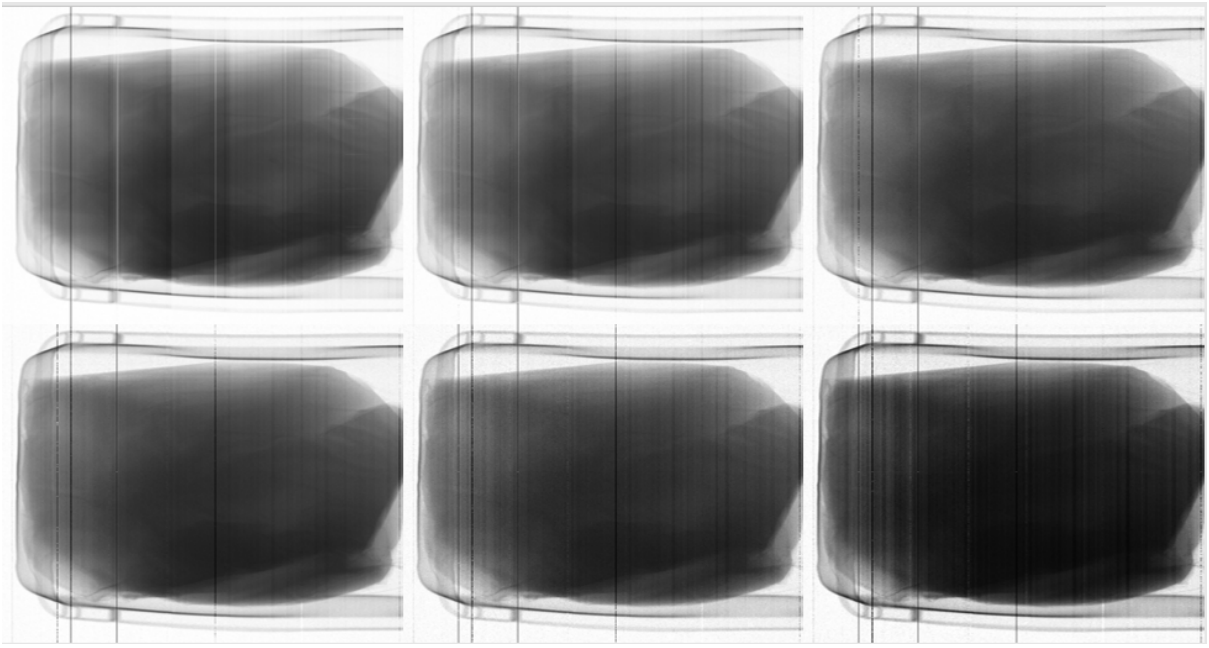

Figure 16: Multi-energy X-ray scan of liver shown at varying greyscale contrast.

The next phase in this work is to map anatomy from the physical dissection back to the X-ray image data in order to mark-up the X-ray image data with the region where the fluke worm is present. This data can then be provided to the Rapiscan algorithm team to start the process of developing an automated algorithm for automatic identification of fluke worm in liver. For this process to result in a high detection rate with low nuisance alarm rate, a considerable number of livers with fluke worm will need to be imaged, analysed and marked up. Suitable image normalisation methods will be required to highlight the fluke worm region for easy confirmation by a veterinary inspector in an abattoir.

A series of hyperspectral scans of the same liver sample were conducted to assess the spectral data obtained from liver. The objectives being:

1. To determine the presence of liver as opposed to any other tissue
2. To determine the state of the liver (diseased or normal).

Figure 17 and Figure 18 show visible wavelength hyperspectral camera imaging of the liver sample on both the upper face and on the lower face. The lower face had been in contact with fluids on the base of the tray and so was damp compared to the top face.

The shape of the hyperspectral data is similar in both cases and is markedly different to the shape of the QIR light source spectrum shown in Figure 1. The reflectivity of the damp surface is higher than the reflectivity of the dry surface and this may provide some useful clinical information in subsequent data analysis.

This project is supported by funding from the Australian Government Department of Agriculture, Water and the Environment as part of its Rural R&D for Profit programme in partnership with Research & Development Corporations, Commercial Companies, State Departments & Universities.

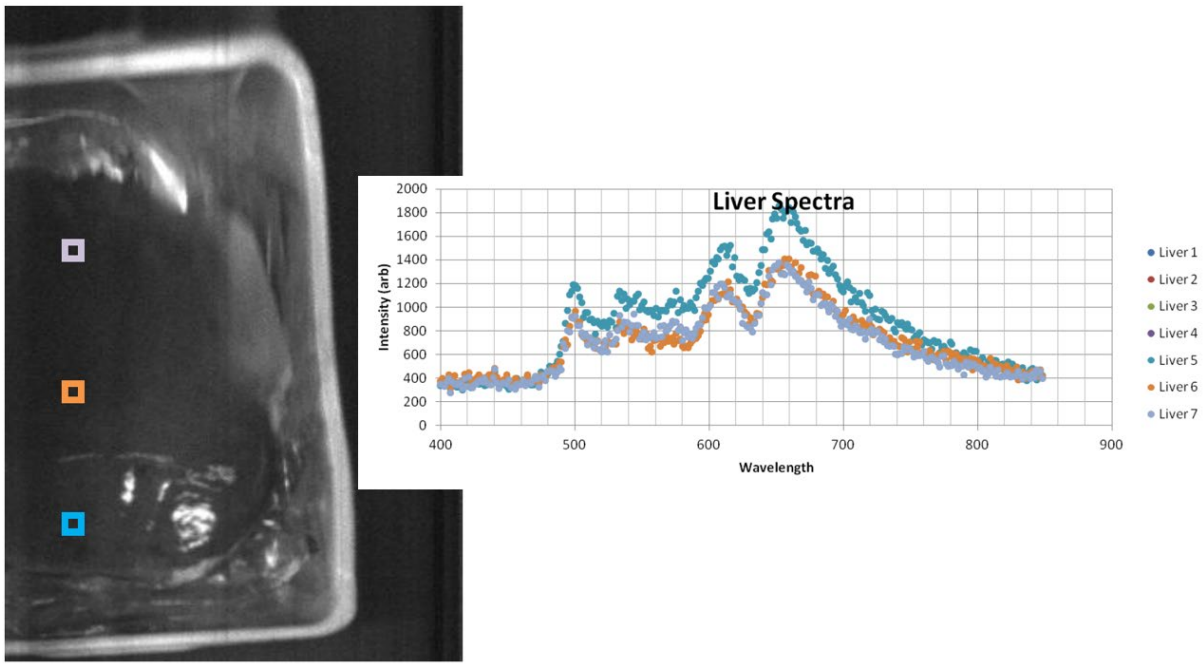

Figure 17: Visible waveband hyperspectral image data of Wagyu beef liver viewed from the upper, dry, face.

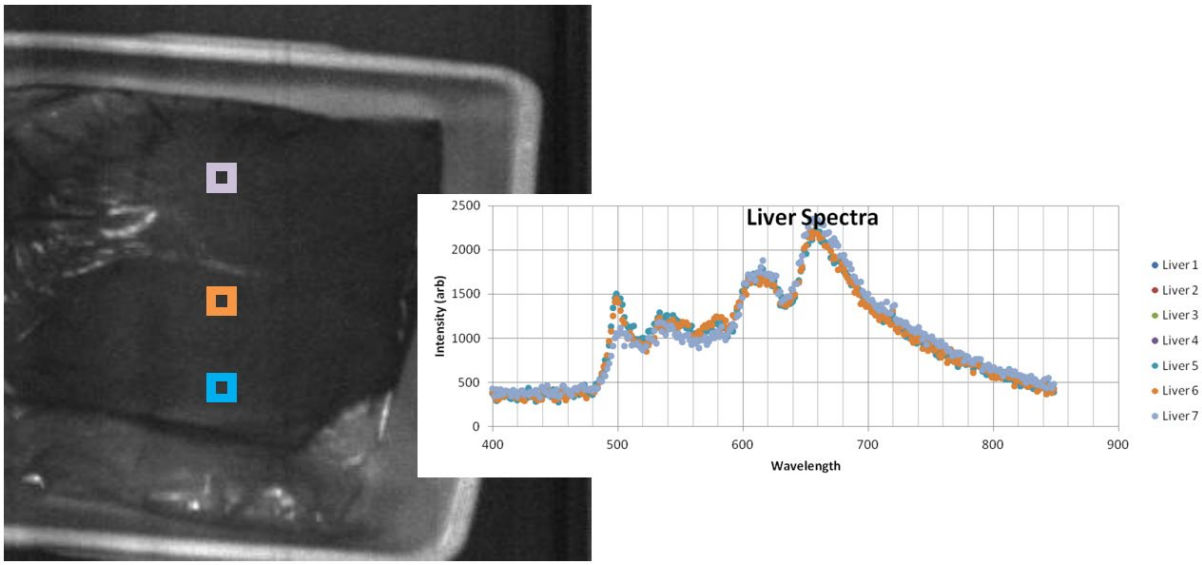

Figure 18: Visible waveband hyperspectral image data or Wagyu beef liver viewed from the rear, damp, face.

3.2.3 Lamb Liver

Figure 19 shows visible waveband spectral data for a lamb liver in both the liver region and in the fat region above the liver. The liver spectral signature is quite similar to the beef spectral signature shown in Figure 17 and Figure 18 while the fat signature is substantially different. This suggest that there may be characteristics of liver in both beef and lamb that correlate in the visible hyperspectral wavelength band. This is data that will need to be explored in more detail during the forthcoming veterinary program.

This project is supported by funding from the Australian Government Department of Agriculture, Water and the Environment as part of its Rural R&D for Profit programme in partnership with Research & Development Corporations, Commercial Companies, State Departments & Universities.

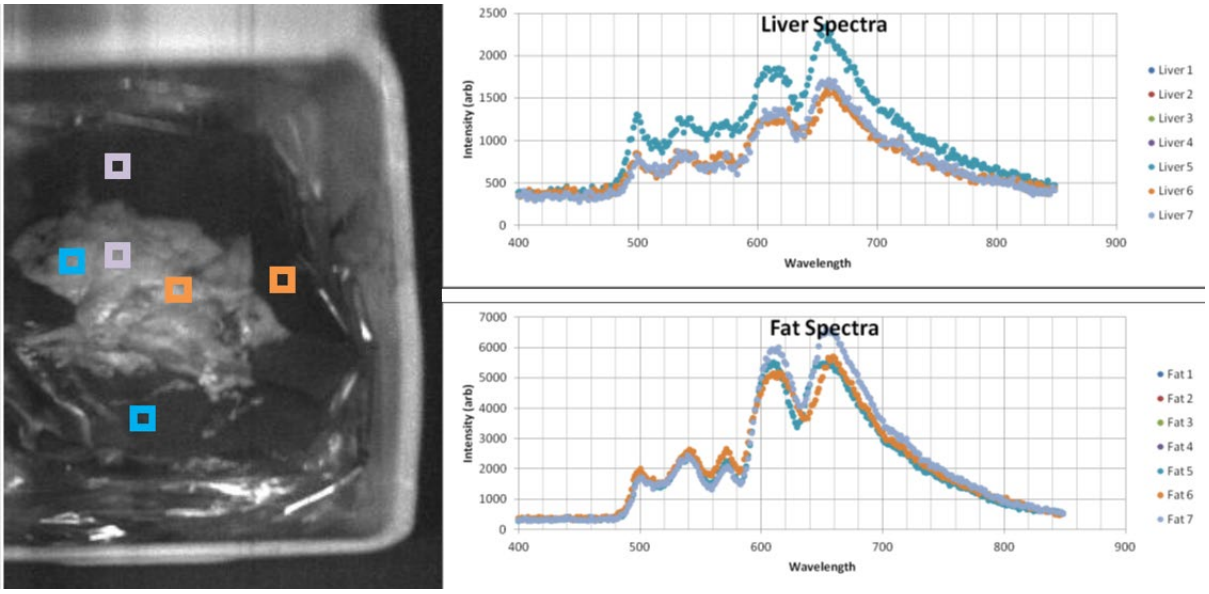

Figure 19: Visible waveband analysis of lamb liver in liver tissue and fat regions.

To further explore differences between different tissue types, a series of different tissues and offal types were scanned using both visible and SWIR hyperspectral regions.

3.2.4 Other Offal Comparison

Figure 20 shows visible waveband hyperspectral camera data for three selected offal samples, liver (upper), heart and kidneys (lower), with pseudo colour (left) and greyscale colour (right). Analysis points are shown with the small coloured rectangles. Data corresponding to each of these rectangles is shown in Figure 21. A qualitative inspection of the four graphs presented in Figure 21 show significant differences between tissue types and the background region of the tray that the samples were contained within. This shows good promise for automatic and reliable identification of offal in the abattoir setting from which more detailed analysis can be conducted on a tissue specific basis using both X-ray and hyperspectral camera data.

Figure 20: Visible waveband images of offal samples. Left: pseudo-colour image. Right: Showing data analysis regions. The data is from two separate scans of the same samples.

This project is supported by funding from the Australian Government Department of Agriculture, Water and the Environment as part of its Rural R&D for Profit programme in partnership with Research & Development Corporations, Commercial Companies, State Departments & Universities.

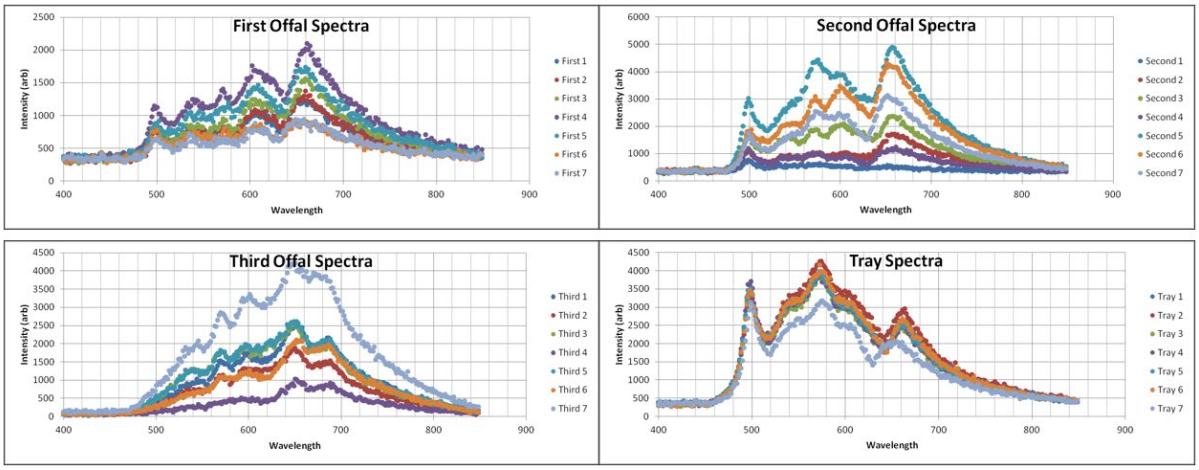

Figure 21: Visible waveband hyperspectral data for different offal types.

Figure 22 shows pseudo-colour and greyscale image data for the same tissue samples in the hyperspectral SWIR wavelength region. Figure 23 shows the tissue spectra at the regions highlighted by the coloured rectangles in Figure 22. Again, a qualitative inspection of these results show promise for automatic identification of tissue type in the abattoir setting.

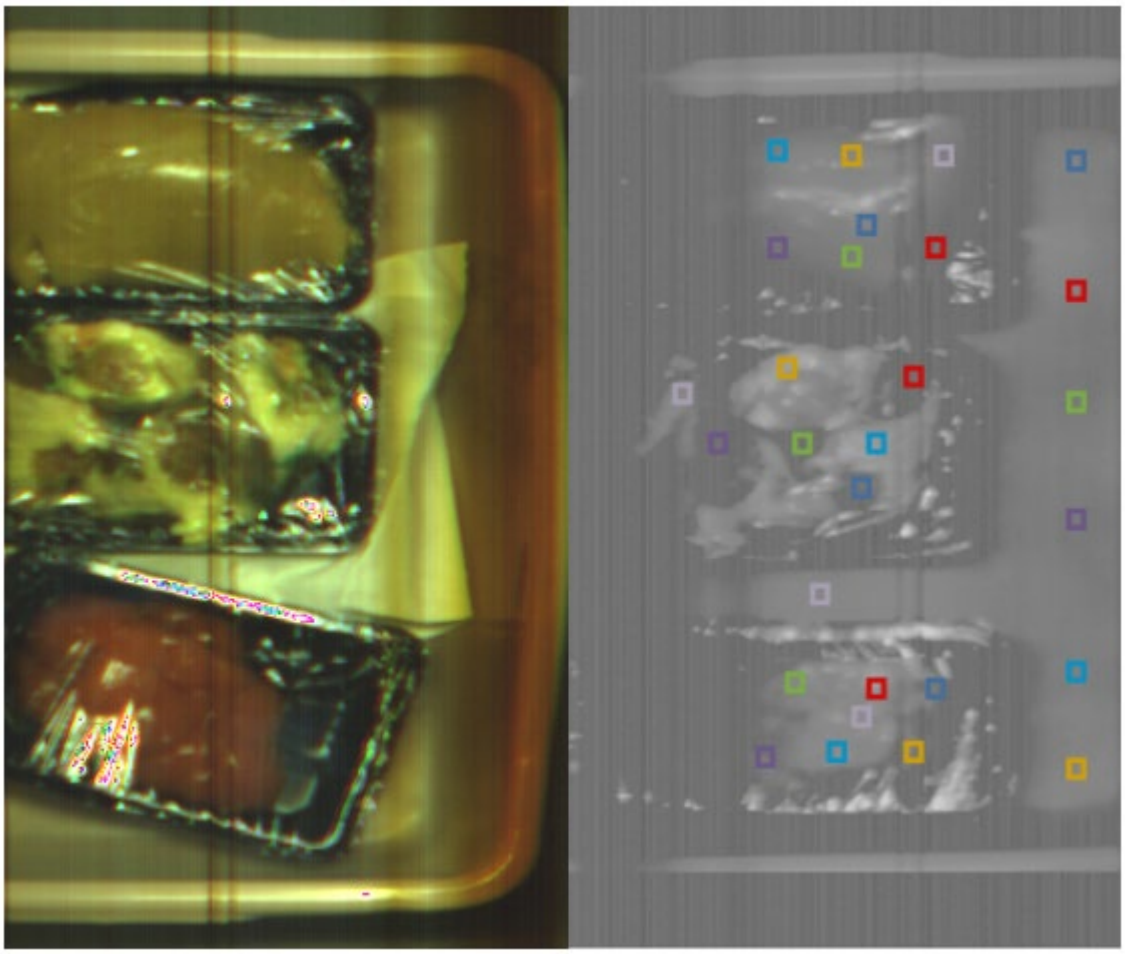

Figure 22: False-colour SWIR hyperspectral image and associated greyscale image with data sampling points shown as coloured squares. The image data comes from two different scans of the same samples. The samples are liver (upper), heart (centre) and kidneys (lower).

This project is supported by funding from the Australian Government Department of Agriculture, Water and the Environment as part of its Rural R&D for Profit programme in partnership with Research & Development Corporations, Commercial Companies, State Departments & Universities.

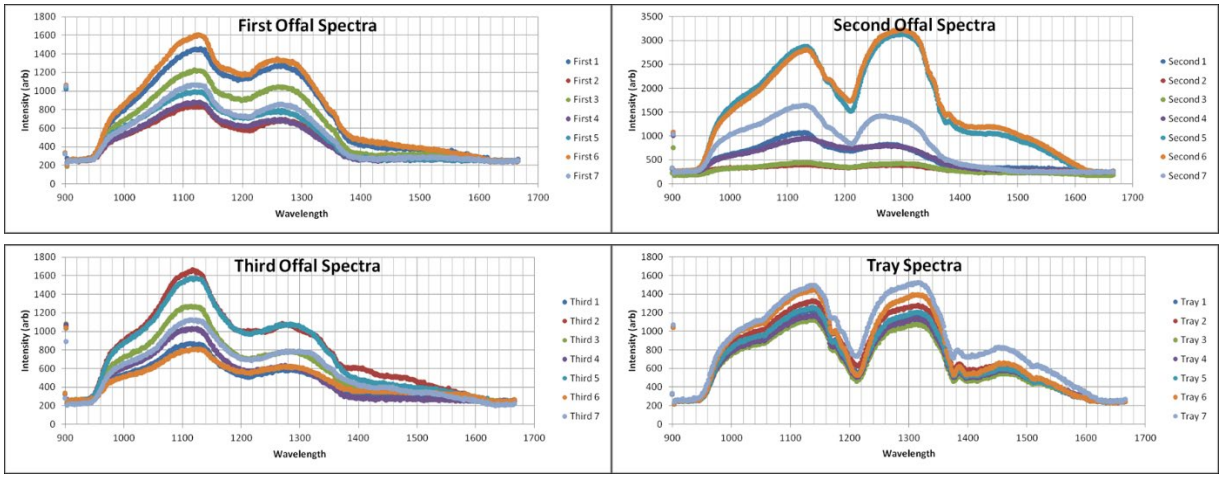

Figure 23: SWIR hyperspectral camera data for offal samples and the tray containing the samples.

Going forwards, the Rapiscan algorithm team will start to conduct a quantitative analysis of these tissue specific spectra once more data has been collected to allow statistical differences between individual animal tissues and to take into account system stability.

3.2.5 Lamb Lung

The University of Sydney team have also conducted some scanning of lamb lungs. Example of MEXA image data is presented in Figure 24. Other than the vertical stripe artefact for which a Rapiscan program is underway to resolve, the image data provides nice contract between airways and lung tissue and suggests the potential for investigating topics such as pneumonia.

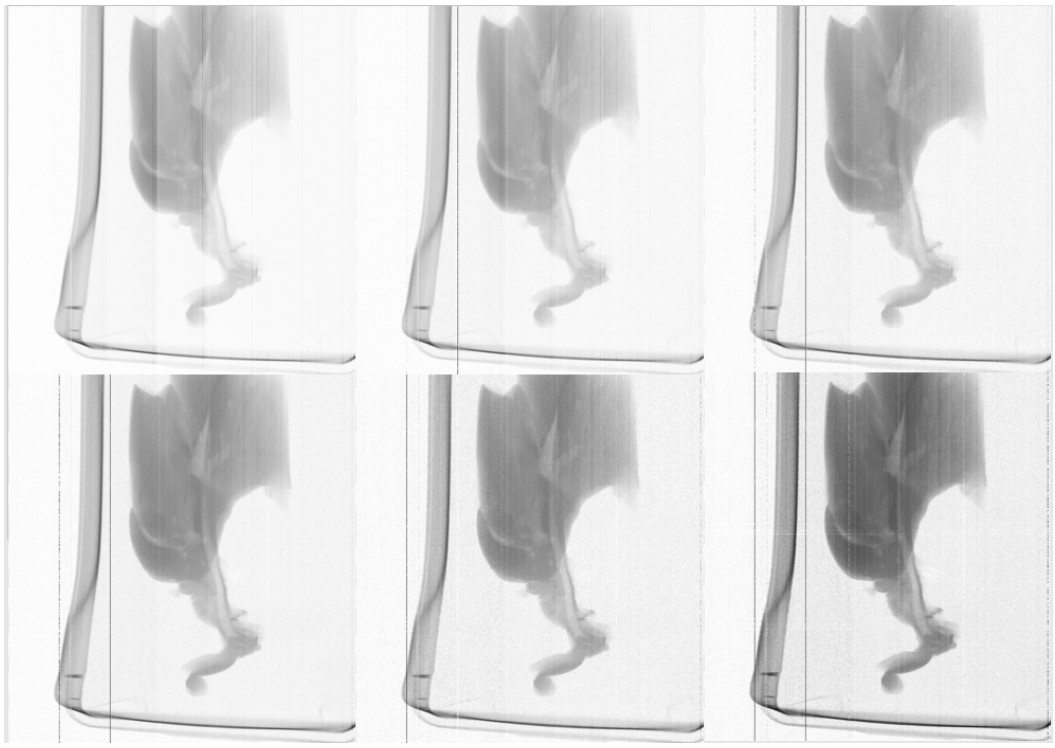

Figure 24: Multi-energy X-ray scan of lamb lungs shown at varying greyscale contrast.

This project is supported by funding from the Australian Government Department of Agriculture, Water and the Environment as part of its Rural R&D for Profit programme in partnership with Research & Development Corporations, Commercial Companies, State Departments & Universities.

3.2.6 Cheesy Glands

Another issue of importance in the abattoirs is the detection of cheesy glands. Example photographs of cheesy glands in mutton (closed and opened) are shown in Figure 25. These mutton trim samples were provided to the program by the Gundagai abattoir. The samples have been scanned and data analysis is currently under progress.

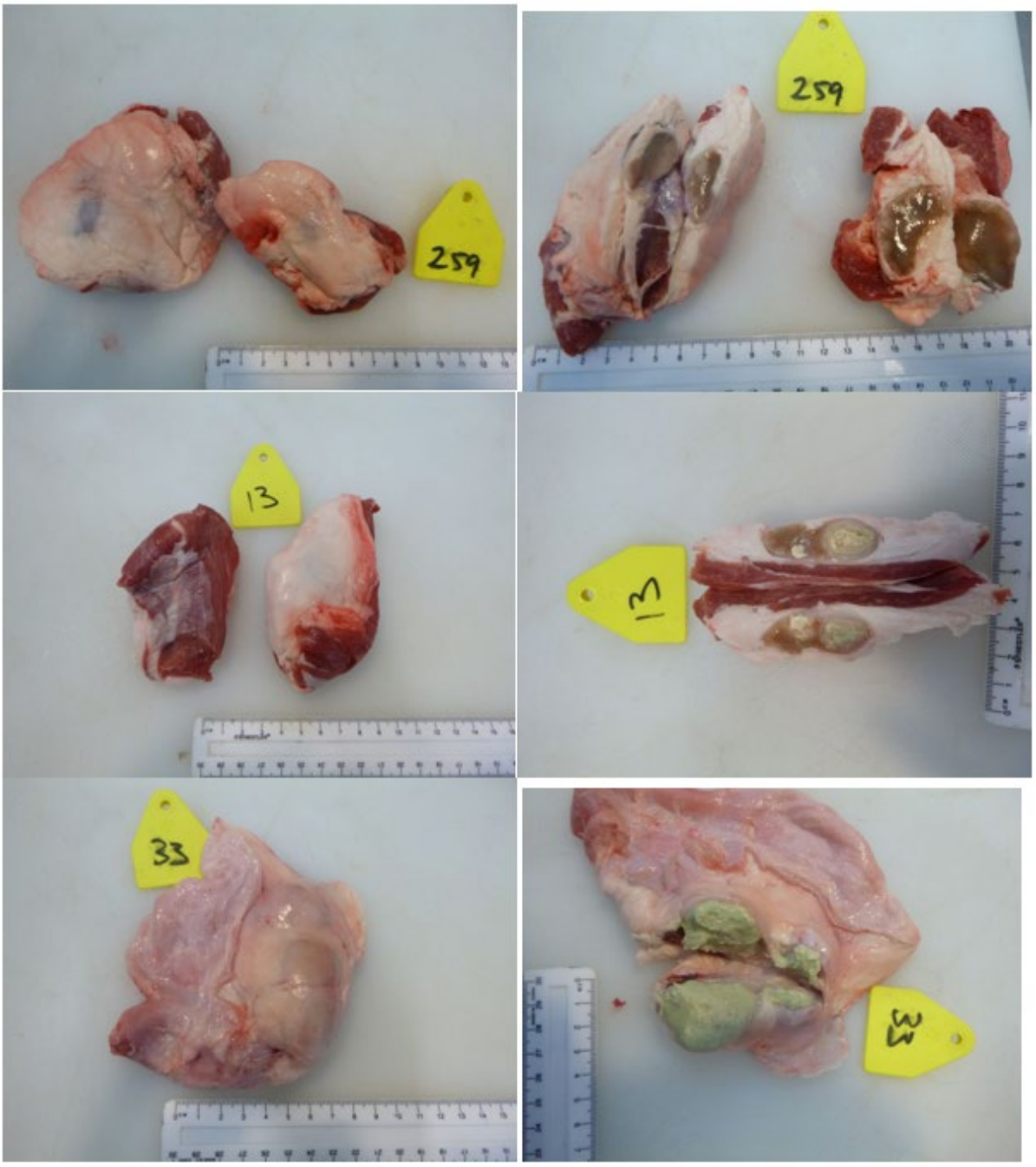

Figure 25: Trims from mutton acquired from the Gundagai abattoir showing cheesy glands (caseous lymphadentis).

This project is supported by funding from the Australian Government Department of Agriculture, Water and the Environment as part of its Rural R&D for Profit programme in partnership with Research & Development Corporations, Commercial Companies, State Departments & Universities.

3.2.7 Whole Animal Imaging

To support the University of Sydney MDC project P.PSH.0817, some X-ray imaging has been conducted on dead lambs. Sample X-ray image data of two lambs is provided in Figure 26. Further work on this recent data will be required to draw further conclusions but the intrinsic image quality looks reasonable for analysis of health issues such as pneumonia, brain inflammation, foreign body inclusions (e.g. syringe needles) and other gross anatomy issues.

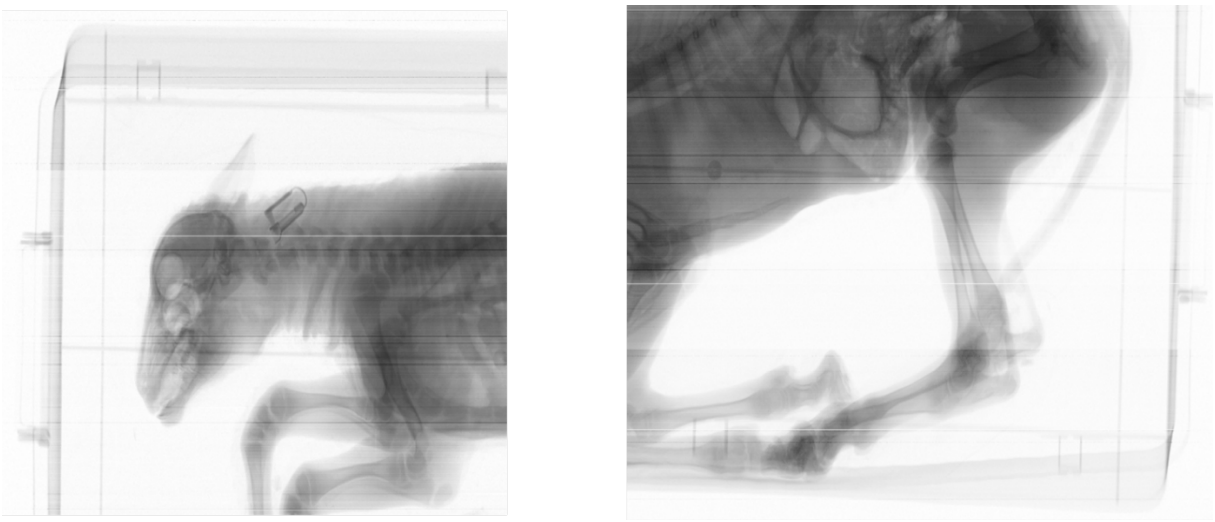

Figure 26: MEXA lamb images acquired in two separate scans and each shown at a different greyscale contrast. The lambs are part of MDC project P.PSH.0817.

3.3 Automated Analysis Algorithms

Based on the preliminary scan data collected to date, it appears that there is good scope for automated algorithms to address a number of key issues:

1. Shape based identification of anatomy
2. Hyperspectral signature identification of individual organs
3. Hyperspectral signature detection of anomalies on individual organs
4. MEXA based identification of specific health issues such as pneumonia.

Working collaboratively with all parties, a more comprehensive data collection and veterinary analysis process for a limited number of heath issues, such as detection of cheesy glands or specific identification of heart, lungs, liver etc, will be required to build up the data library from which real algorithm development can start.

To supplement the data that can be obtained from the MEXA and hyperspectral data, additional information can be collected from the abattoir in real-time, for example using RFID based lookup of data from a central database. This data could usefully include information such as animal type, age, weight and farming/feeding methods.

The goals for the automated algorithm methods are to:

1. Determine, automatically, which organ or offal types are present in the scanned image data

This project is supported by funding from the Australian Government Department of Agriculture, Water and the Environment as part of its Rural R&D for Profit programme in partnership with Research & Development Corporations, Commercial Companies, State Departments & Universities.

2. Generate an electronic report for each organ or offal type to describe any known disease or defects that have been identified in each particular item that has been scanned
3. Generate a report to summarise the health status of all organs and offal from a particular animal to include an overall health risk rating for that animal.

Based on the experimental program to be conducted by the University of Sydney team, supported by Rapiscan Systems, it is planned to analyse both offal and shelf-ready product in its finished packing. This will allow a feasibility assessment to be conducted for finished product quality control using MEXA plus hyperspectral imaging

This project is supported by funding from the Australian Government Department of Agriculture, Water and the Environment as part of its Rural R&D for Profit programme in partnership with Research & Development Corporations, Commercial Companies, State Departments & Universities.

4 A preliminary investigation into the automatic detection of diseased sheep organs using hyperspectral imaging

Cassius E.O. Coombs[*, #], Brendan E. Allman[†], Edward J. Morton[%], Marina Gimeno[‡], Neil Horadagoda[‡], Garth Tarr[§], Luciano A. González[*]

* Sydney Institute of Agriculture and School of Life and Environmental Sciences, Faculty of Science, The University of Sydney, NSW 2570, Australia.

† Rapiscan Systems Pty Ltd., Melbourne Airport, VIC 3045, Australia.

% Rapiscan Systems Pte Ltd., Singapore 348574, Singapore.

‡ University Veterinary Teaching Hospital Camden, Sydney School of Veterinary Science, Faculty of Science, The University of Sydney, NSW 2570, Australia.

§ Faculty of Mathematics and Statistics, The University of Sydney, NSW 2006, Australia.

Corresponding author: cassius.coombs@sydney.edu.au

This project is supported by funding from the Australian Government Department of Agriculture, Water and the Environment as part of its Rural R&D for Profit programme in partnership with Research & Development Corporations, Commercial Companies, State Departments & Universities.

Abstract

The post-mortem inspection process of livestock viscera at abattoirs is expensive and gruelling, but it is essential for the detection and condemnation of edible organs and carcass due to food safety issues. Lesions in hearts, kidneys, livers, and lungs are amongst the most common offal defects found in abattoirs. Visible (VIS) and short-wave infrared (SWIR) hyperspectral imaging implemented in a multisensory platform were used to differentiate between sheep parenchymatous organs passed as fit (Healthy, n = 42) or not fit (Diseased, n = 47) for human consumption. Partial least squares discriminant analysis (PLS-DA) and random forest (RF) were used to classify organs as healthy or diseased in heart (n = 28), kidney (n = 15), liver (n = 24), and lung (n = 22). PLS-DA produced equal or greater classification accuracy and sensitivity than RF for all organs except for lung when VIS sensors were used (means 84.4% and 78.3%, respectively). Livers and hearts (86.9%) showed higher accuracy than lungs and kidneys (75.9%). Limited differences occurred between VIS and SWIR sensors, although only one sensor tended to be more accurate compared to a combination of both. SWIR outperformed VIS in accuracy across all organs (84.8% vs. 76.3%), and the combination of VIS and SWIR was also accurate (83.0%). The use of hyperspectral imaging is an attractive proposition for the meat processing industry as a non-invasive imaging technology to detect defects in offal, and it can also provide automatic detection, saving time and labour costs.

Keywords: disease detection, automation, meat processing, sheep health, discriminant analysis, organ condemnation, inspection

This project is supported by funding from the Australian Government Department of Agriculture, Water and the Environment as part of its Rural R&D for Profit programme in partnership with Research & Development Corporations, Commercial Companies, State Departments & Universities.

Introduction

The automation of the post-mortem meat and animal product inspection and processing in the abattoir has been sought for a long time. One such area of automation has been the sortation of offal based on fitness for human consumption via the detection of defects, contamination, or infectious disease (Thomas-Bachli et al., 2014; Webber et al., 2012). In the abattoir, such examinations are carried out by meat inspectors under the supervision of a veterinarian (Webber et al., 2012; Wilson et al., 2019). This inspection is of vital public health importance due to the removal of potential zoonotic diseases from the processing chain and thereby limiting human exposure (Butler et al., 2003). In addition, this inspection has economic benefits in surveillance of diseases and providing feedback to producers, which could be made quicker with automation (Thomas-Bachli et al., 2014). Furthermore, previous research in sheep found correlation between lung lesions (pleuritis, abscessation and pneumonia) with reduced daily gain, reduced carcase fat, and longer time to reach optimal carcase weight, which along with potential condemnation, affect returns to producers (Goodwin-Ray et al., 2008; Jones et al., 1982; Lacasta et al., 2008). These findings highlight the economic benefits of automatic detection and rapid reporting of animal health to producers.

In recent decades, automation in the meat processing industry has become prevalent (Nade et al., 2005; Scholz et al., 2015; Toohey et al., 2018). Similarly, veterinary medicine studies have used computed tomography (CT) to detect abnormalities in

This project is supported by funding from the Australian Government Department of Agriculture, Water and the Environment as part of its Rural R&D for Profit programme in partnership with Research & Development Corporations, Commercial Companies, State Departments & Universities.

anaesthetised cattle prior to euthanasia and organ removal (Lee et al., 2009; Lee et al., 2011). The use of modern non-contact sensor technology to automate the process of meat and offal inspection to detect health and safety hazards has been suggested, with expectations to provide a more rapid, accurate, and sensitive measurement, with greater maintenance of food safety (Neethirajan et al., 2017; Uzal et al., 2002; Webber et al., 2012). Sensors also provide automatic decision making and sorting tools for characterisation and deviation detection in processing plants (Neethirajan et al., 2017). Non-invasive inspection can also prevent potential spread of zoonotic diseases or cross-contamination of infectious diseases between carcases or organs (Samuel et al., 1980; Uzal et al., 2002). Despite this, the post-mortem scanning of internal organs has been scarce, with high costs and practicality affected by the physical size of imaging systems presenting constraints to their commercial uptake (Neethirajan et al., 2017; Scholz et al., 2015; Webber et al., 2012). Similarly, image size and the low speed of computers present a constraint when a large number of organs need to be scanned on a commercial production line (Coombs et al., 2021; Elmasry et al., 2012a).

The use of hyperspectral (HS) imaging, which can be split into visible (VIS: 400-900 nm) and short-wave infrared (SWIR: 900-1700 nm), has been successfully trialled previously to detect microbial spoilage in fish (Cheng and Sun, 2015), skin tumours in poultry (Nakariyakul and Casasent, 2009), and offal contamination in meat mixtures (Kamruzzaman et al., 2014). The latter studies all showed precision and accuracy greater than 90%. The suitability of hyperspectral imaging for the meat and food industries has been the subject of several reviews (Baeten et al., 2007; Elmasry et al., 2012a; Huang et al., 2014; Xu and Sun, 2017). Prediction algorithms can be developed to differentiate animal tissues and abnormalities from measurements of size, texture, colour, shape, and spectral signatures of regions of

This project is supported by funding from the Australian Government Department of Agriculture, Water and the Environment as part of its Rural R&D for Profit programme in partnership with Research & Development Corporations, Commercial Companies, State Departments & Universities.

interest (ROI) (Elmasry et al., 2012a; Xu and Sun, 2017). However, none of these reviews examined HS sensor technology as a tool to detect diseases in sheep organs.

Diseases commonly encountered post-mortem in parenchymatous organs in include liver fluke (*Fasciola hepatica*) and cysticercosis (*Cysticercosis tenuicollis*) in the liver, caseous lymphadenitis (CLA; *Corynebacterium pseudotuberculosis*) and pneumonia (*Pasteurella spp.* and *Mycoplasma spp.*) in lungs, cysticercosis (*Cysticercus ovis*) in the heart, and interstitial nephritis in the kidney (AHDB, 2017). In addition, hydatid cysts (*Echniococcus granulosis*), abscesses, and haemorrhage can occur in several organs. These animal health issues lead to condemnation of the organ for human consumption and may even result in condemnation of the entire carcase. For instance, the carcase is usually condemned if *C. ovis* cysts are found in three or more locations, or if emaciation occurs concurrently with liver cysts or CLA, or secondary infections such as septicaemia occur from pneumonia (AHDB, 2017). Poor body scores and excessive abscessation can also lead to entire carcase condemnation, which result in significant economic losses (Arsenault et al., 2003; Uzal et al., 2002).

The present study selected parenchymatous organs (hearts, kidneys, livers, and lungs) from sheep that were and were not deemed fit for human consumption by the inspectors at a commercial abattoir. Organs were scanned using a multisensory platform encompassing VIS and SWIR sensors, and then examined grossly by veterinary pathologists to confirm abnormalities. These spectral data were then analysed using both partial least squares discriminant analysis (PLS-DA) and random forest (RF) as per Coombs et al. (2021) to classify each organ as healthy or diseased. It was hypothesised that both PLS-DA and RF would have good and comparable accuracy in classifying the organs as healthy or diseased.

This project is supported by funding from the Australian Government Department of Agriculture, Water and the Environment as part of its Rural R&D for Profit programme in partnership with Research & Development Corporations, Commercial Companies, State Departments & Universities.

Materials and Methods

All offal used in the present study were sourced from a collaborating abattoir and animal ethics approval was not necessary.

Sample collection and storage

A total of 89 sheep parenchymatous organs were collected from a collaborating abattoir in New South Wales, Australia, following commercial slaughter. Organs were processed as per Australian guidelines including palpation and incisions if needed (Wilson et al., 2019) and were stored chilled (1-4 °C) when not examined or scanned. Organs were described as hearts, kidneys, livers, or lungs, and either healthy or diseased, with those diseased considered as not fit for human consumption (Table 1). All organs were transported from the abattoir to the laboratory, scanned entire with the multisensory platform, and then examined for abnormalities by experienced veterinary pathologists.

Scanning procedure

All organs were scanned using a multisensory scanning platform encompassing HS technology and multi-energy X-ray attenuation (Rapiscan Inspection System AK198, Rapiscan Systems Pty Ltd., Torrance, CA) as previously described by Coombs et al. (2021). The multisensory system included a conveyor belt (6.64 s, 1260 mm, 0.19 m/s) and it was run by an Ubuntu (Linux) Cube computer program, which controlled exposure time, image size, and acquisition rate. Two HS sensors covered the spectral range from 400 to 900 nm (VIS) and 900 to 1700 nm

This project is supported by funding from the Australian Government Department of Agriculture, Water and the Environment as part of its Rural R&D for Profit programme in partnership with Research & Development Corporations, Commercial Companies, State Departments & Universities.

(SWIR). The VIS (Basler Ace GigE, Photonic Science, East Sussex, UK) and SWIR (Snake A/C GigE v3 AK081, Photonic Science, East Sussex, UK) sensors were powered by 12 V power supply units and fitted with Specim spectrographs (VNIRV10E and NIR V17E, respectively) and a Grade 1 InGaAs detector with air cooled housing. Spectral resolutions were 3 and 5 nm for VIS and SWIR, respectively, with both sensors capturing 200 spectral slices per second. Spectral increment (1.5 nm, VIS 300 bands, and SWIR 512 bands), sensor resolutions (VIS 1920 x 1200 px; SWIR 640 x 512 px), frame rate (150 fps), refresh rate (150 Hz, 6.66 ms) and exposure times (VIS 6.4 ms; SWIR 4.0 ms) were used as per Coombs et al. (2021).

Organs' gross examination

All organs were systematically examined by veterinary pathologists for gross lesions. Should a lesion be present the following data were recorded: location, distribution, demarcation, colour, shape, appearance of the cut surface, and consistency. The most likely cause of the lesion was also recorded to the organ in question. Organs were also examined for off-colours and inconsistency in texture by palpation, with sectioning and sampling for histopathology in some instances, to confirm the identity of the lesions.

Image analysis and extraction of spectral data

As per Coombs et al. (2021), hyperspectral images (both VIS and SWIR) were downloaded as 200-300 slices in PNG format, with trimming done to remove slices beyond 10 frames either side of the tray the samples were scanned in. MATLAB programming language (MATLAB R2021a, Mathworks Inc., USA) was used to construct complete organ images from individual

This project is supported by funding from the Australian Government Department of Agriculture, Water and the Environment as part of its Rural R&D for Profit programme in partnership with Research & Development Corporations, Commercial Companies, State Departments & Universities.

frames, with these images viewed using Gnu Image Manipulation Program (GIMP) software (version 2.10.18; GIMP Development Team, 2020) and marked-up using ImageJ (version 1.53a; National Institutes of Health, Bethesda, MD). Three to eight evenly spaced ROI (7 x 7 px, 10.2 mm width x 9.0 mm length) were marked-up for each organ depending on the size of the organ. Pixel dimensions of the ROI were written into a MATLAB algorithm to extract spectral data. All HS data (both VIS and SWIR) were averaged for each organ, with organs classified by their organ type (heart, kidney, liver, or lung) and their status (Diseased or Healthy, based on the classification at the abattoir and corroborated by the pathologists).

Outlier removal and spectral trimming

Subsequently, mean reflectance spectral data from VIS, SWIR, and combination of both sensors (COMB) were imported into R (version 4.0.2; R Core Team, 2020). A principal components analysis (PCA) model using the *mdatools* package (Kucheryavskiy, 2020) was used to visualise each dataset and identify outliers with orthogonal and score distances > 20 on the Q residual plot (Kucheryavskiy, 2021). Two organs (one diseased heart and one diseased lung) were removed from the VIS and COMB datasets because these were detected as outliers. As per the data pre-processing methods of Coombs et al. (2021), the spectra between 470.5 and 800.5 nm (VIS), and 1000.5 and 1600.5 nm (SWIR) were retained with those outside these ranges presenting as flat endpoints.

In the present study comparisons were made between the disease statuses of different organs, therefore all datasets (VIS, SWIR, and COMB) were analysed separately according to their organ type (heart, kidney, liver, and lung). As per the results obtained by

This project is supported by funding from the Australian Government Department of Agriculture, Water and the Environment as part of its Rural R&D for Profit programme in partnership with Research & Development Corporations, Commercial Companies, State Departments & Universities.

Coombs et al. (2021), all reflectance spectra were smoothed using the trimmed centred moving average method with a sliding window (length = 11) and then transformed to obtain the first derivative of absorbance where absorbance = log(1/reflectance). All data processing was done in R (R Core Team, 2020) with the assistance of the suite of *tidyverse* packages (Wickham et al., 2019).

Classification model development

Classification models were developed using two machine learning methods within the *Caret* package (Kuhn, 2021) i.e., partial least squares discriminant analysis (PLS-DA) and random forest (RF). Resampling for model tuning and evaluation of all datasets was done using the leave-one-out cross validation (LOOCV) method and all datasets were centred and scaled. The number of components (*ncomp*) for PLS-DA models of each organ type were selected according to the highest accuracy. The number of variables available for splitting at each tree node (*mtry*) used for the RF models was selected using the lowest log loss (Kuhn, 2008; Liaw and Weiner, 2002).

Model evaluation for diseased or healthy status was done by fitting tuned models using the LOOCV of each of the four organ types, three spectral ranges, and both classification methods. For the estimated models, goodness-of-fit model metrics including sensitivity, specificity, precision, accuracy, and coefficient of agreement (Kappa) were generated with Diseased being the positive class.

Results

This project is supported by funding from the Australian Government Department of Agriculture, Water and the Environment as part of its Rural R&D for Profit programme in partnership with Research & Development Corporations, Commercial Companies, State Departments & Universities.

Abattoir sortation and post-mortem

All organs labelled by the abattoir as healthy or fit for human consumption (n = 42), were similarly labelled by the veterinary pathologists with no detectable lesions. However, 16 of the 47 organs labelled as diseased at the abattoir presented no detectable gross lesions other than discolouration and were therefore rejected for human consumption (Table 1). Discolouration was the most common and predominant reason for rejection of hearts and kidneys (73.7%), whereas mineralisation in the liver (36.4%), CLA (35.3%) and pneumonia (29.4%) in lungs were also significant in the present study (Table 1).

Spectral data and model tuning

Figs. 1 and 2 show the transformed VIS and SWIR absorbance spectra, respectively, split by organ type. The VIS spectra showed no complete separation of diseased organs from healthy organs (Fig. 1). However, the region between 600 and 660 nm showed the greatest separation between healthy and diseased status, particularly for hearts and livers, with diseased organs showing greater absorbance than healthy organs at 600 to 620 nm, and the reverse occurring from 620 to 660 nm. The SWIR spectrum of organs showed a more evident and longer region of healthy and diseased organ differentiation than VIS (1020-1320 nm), regardless of organ type (Fig. 2). Across this range, the clearest differentiation between healthy and diseased organs occurred in kidneys, where absorbance was greater for healthy than diseased kidneys.

Due to the small sample size, *ncomp* of the PLS-DA models tended to be small, particularly for liver and lung, with lung being the most unbalanced organ dataset in terms of numbers of healthy and diseased (Table 2). Conversely, heart was the most abundant organ, and all PLS-DA models used *ncomp* of 5 or more (Table 2). It is worth noting that *ncomp* of 10

This project is supported by funding from the Australian Government Department of Agriculture, Water and the Environment as part of its Rural R&D for Profit programme in partnership with Research & Development Corporations, Commercial Companies, State Departments & Universities.

was originally selected for COMB differentiation of liver, although this model overfit with 100% for all goodness-of-fit metrics on the training dataset but much lower on the validation dataset (data not shown). The smallest organ in total number (kidney) had the lowest *mtry* values for SWIR, though the highest for VIS and COMB. Meanwhile, the most abundant (heart) had the greatest *mtry* values for SWIR, and the lowest for COMB (Table 2).

Classification of organs as healthy or diseased

Table 2 shows the results for differentiating sheep organs based on healthy or diseased status using three different spectra (VIS, SWIR, and COMB) and two different classification methods (PLS-DA and RF). Hearts and livers were correctly classified as diseased or healthy using PLS-DA above 85% regardless of the sensor used. All diseased lungs were correctly identified as diseased using SWIR and PLS-DA, whereas all healthy kidneys were correctly identified as healthy using the same methods. The combination of the two sensors predicted disease status better than both individual sensors with PLS-DA modelling for livers, and with RF modelling for hearts. However, COMB did not outperform both individual sensors for any other organ or classification method.

Classification and detection of diseased kidneys tended to be the weakest among the organs used in the present study, showing sensitivities below 67% and accuracies below 87%. In contrast, lungs showed the lowest specificity across sensors and models with RF modelling below 20% and Kappa below 18%.

Regarding machine learning methods, PLS-DA outperformed RF in classification accuracy except for differentiating healthy and diseased lungs using the VIS sensor (Table 2).

This project is supported by funding from the Australian Government Department of Agriculture, Water and the Environment as part of its Rural R&D for Profit programme in partnership with Research & Development Corporations, Commercial Companies, State Departments & Universities.

However, the majority of these differences were small or RF was equal in accuracy to PLS-DA, which occurred for differentiating healthy from diseased hearts using COMB and livers using SWIR.

Discussion

In examination of the organs, it was determined that CLA was the most common disease of sheep resulting in offal rejection for human consumption in the present study (35.3%), which was consistent with Australian sheep findings reported by Webber et al. (2012). Pneumonia and CLA made up the majority of rejected lungs (64.7%), whereas the most common disease for rejected livers was focal parenchymal mineralisation (36.4%). On the other hand, most of the condemned hearts and kidneys in the present study were rejected due to discolouration. From a food safety perspective, CLA dominance provides limited risk to the entire carcase (Murray, 1986) or human health if there are no open wounds (Arsenault et al., 2003). However, labour associated with slicing to detect CLA lesions and abscesses, carcase trimming, and disinfection, has been mentioned as associated losses for processors, along with reduced performance and animal deaths for producers (Arsenault et al., 2003). For this reason, the automatic detection and subsequent excision of CLA lesions could enhance the post-mortem process.

The measurement of instrumental colour (Commission International l'Eclairage L*, a*, b*) and detection of its changes have been previously explored using HS imaging and computer vision (Chen and Kim, 2004; Elmasry et al., 2012b; Xu and Sun, 2017). For instance, long-wave NIR HS (964 to 1631 nm) was used successfully with instrumental colorimetry to

This project is supported by funding from the Australian Government Department of Agriculture, Water and the Environment as part of its Rural R&D for Profit programme in partnership with Research & Development Corporations, Commercial Companies, State Departments & Universities.

measure colour changes in salmon fillets (Wu et al., 2012). Such technologies could be similarly applied using different organs, although the colorimeter would provide contact with the organs. Hyperspectral analysis can detect different surface textures within the same organ (Xu and Sun, 2017), which could assist with identifying specific regions of disease such as CLA within an organ, and also detect specific diseases that may be present. However, more samples would be required to develop a reliable training model that can be evaluated with an independent dataset rather than using resampling as used in the present study. In addition, more samples possessing one particular pathology or lesion type, such as CLA in the mediastinal lymph nodes of the lung (Arsenault et al., 2003; Webber et al., 2012), could also improve the prediction models for identification of specific diseases and locations within organs.

The collection of several condemned organs with similar pathologies may also improve HS prediction models and allow them to detect additional lesions and identify specific diseases and their locations within organs. For instance, CLA in the mediastinal lymph nodes of the lung could be used for this based on the results of the present study and others (Arsenault et al., 2003; Webber et al., 2012). In turn, this could reduce the costs of veterinary inspection in the abattoir, particularly given the lack of zoonotic diseases (e.g., liver fluke) encountered in the present study.

Hyperspectral prediction models were better at detecting diseased than healthy lungs as reflected by the high sensitivity and low specificity. However, this would likely mean healthy lungs would be marked as diseased by the model. The other organs tended to have higher specificity than sensitivity, although the values were much closer than in lungs. These sensitivities showed that, while promising, this system requires substantial improvements (Xu

This project is supported by funding from the Australian Government Department of Agriculture, Water and the Environment as part of its Rural R&D for Profit programme in partnership with Research & Development Corporations, Commercial Companies, State Departments & Universities.

and Sun, 2017). The combination of the two HS sensors spanning visible and short-wave infrared ranges (400-1700 nm) did not necessarily provide greater accuracy than either of the two sensors separately, which was a finding similar to a previous study where the sensors were used to differentiate organs by type (Coombs et al., 2021). Despite the small sample size, the positive goodness-of-fit statistics sorting hearts and livers as diseased or healthy encountered in the present study constitutes a good feasibility study rather than for industry purposes (Williams et al., 2017). However, the use of samples with more gross lesions present may provide greater accuracy and sensitivity, which was true in the present study for livers and lungs, respectively. Larger datasets and more gross lesions could allow for combination with the study by Coombs et al. (2021) to also discriminate between different organ types as well as between healthy and diseased organs, which would be ideal prior to trialling such technologies in abattoirs.

The use of non-invasive imaging devices could assist the biosecurity procedures in preventing diseases bypassing into markets as a result of human error. In this context, studies on breast cancer screening in humans have reported artificial intelligence models as being more accurate in mammogram performance than human screeners (McKinney et al., 2020). However, similar studies using artificial intelligence in animal health surveillance are still in their infancy, though improved accuracy and decision making have been noted (Ezanno et al., 2021). The present study did not attain high accuracy for all organs but provides a solid pilot study encouraging a large-scale study to be conducted. Few studies have taken to imaging animal organs, with most that employed non-invasive imaging devices providing information on whole carcase, meat, or skin composition and health (Elmasry et al., 2012a; Elmasry et al., 2012b; Nade et al., 2005; Scholz et al., 2015). However, some veterinary medicine studies

This project is supported by funding from the Australian Government Department of Agriculture, Water and the Environment as part of its Rural R&D for Profit programme in partnership with Research & Development Corporations, Commercial Companies, State Departments & Universities.

scanned entire live sedated animals scanned with CT for detection of lesions such as abscesses in cattle (Lee et al., 2009; Lee et al., 2011) and screening for cystic echinococcosis in sheep (Mao et al., 2017). Subsequently, animals were euthanised and lesions were examined using histopathology (Lee et al., 2009; Lee et al., 2011; Mao et al., 2017). However, these studies tended to be exploratory in nature with a small number of samples and use of simple regression and Pearson correlation analyses, rather than focusing on surveillance of large numbers of animals entering processing plants with more advanced machine learning modelling.

Regarding machine learning classification methods, PLS-DA tended to be more accurate than RF in the majority of the models, which was also seen in the prior study differentiating beef and sheep organs by type (Coombs et al., 2021). However, the accuracy of RF was not overly lower than PLS-DA and was equal in several models,. Random forest modelling is a more modern and alternative classification method to the conventionally used PLS-DA (Huang et al., 2014; Liaw and Wiener, 2002). Previous findings using RF for classification of rice cultivars (Kong et al., 2013) and in plant ecological studies (Cutler et al., 2007; Lawrence et al., 2006) were positive. However, few studies have employed RF in studies with HS data classifying animal products. In the present study only discrimination of diseased and healthy lungs using VIS showed improved accuracy, sensitivity and precision for RF compared to PLS-DA, with lower specificity and Kappa. Similarly, only kidneys using VIS data showed improved specificity and Kappa for RF compared to PLS-DA, with equal precision and accuracy. Overall, it can be concluded that RF showed promise but was generally lower in accuracy as a machine learning method compared to PLS-DA.

This project is supported by funding from the Australian Government Department of Agriculture, Water and the Environment as part of its Rural R&D for Profit programme in partnership with Research & Development Corporations, Commercial Companies, State Departments & Universities.

It was an interesting finding that hearts were one of the most accurately classified organs for diseased or healthy status given that only 10 of the 13 hearts condemned by the abattoir had evidence of pathological processes at gross examination as opposed to appearance defects. On the other hand, all condemned lungs and the majority of livers had evidence of clinical diseases associated with them. This finding of more gross lesions present in the liver and lungs, resulting in production losses, was demonstrated by previous studies (Arsenault et al., 2003; Mao et al., 2017). Furthermore, Mao et al. (2017) found that the presence of cysts in both livers and lungs of sheep was highly correlated, and that the use of CT on live sheep successfully identified 86% of the total number of cysts found during a necropsy. The CT showed better results for determining the diameter, location and type of cyst. Similar results were found in the present study for sheep livers and lungs using SWIR HS and PLS-DA as a classification method (91-92% accuracy). However, the present study did not identify the size, type or location within the organ of the lesions, which could assist in the extraction of spectral data from the lesions themselves. Therefore, future studies should include an accurate demarcation of the lesion and differentiation by type with larger sample size, which could be further improved with combination of X-ray and HS imaging. In doing so, rapid and objective post-mortem health feedback from processors to producers could be made (Lee et al., 2011; Webber et al., 2012). Hyperspectral imaging could also assist with animal and herd health management post-mortem at a veterinary medicine level (Neethirajan et al., 2017), providing diagnoses and identifying potential disease outbreaks as has been done previously in exploratory studies using CT (Lee et al., 2009; Mao et al., 2017).

Conclusion

This project is supported by funding from the Australian Government Department of Agriculture, Water and the Environment as part of its Rural R&D for Profit programme in partnership with Research & Development Corporations, Commercial Companies, State Departments & Universities.

Visible and short-wave infrared hyperspectral imaging can be used to determine the disease status of sheep organs, with this pilot study proving that classification accuracy was adequate overall and was particularly successful for livers and hearts. However, it is worth noting that the diseases were often identified with the naked eye, palpation, or were presented as discoloured to abattoir inspectors. Future studies could use HS imaging, alone or in combination with other technologies such as multi-energy X-ray or CT, to identify specific pathologies within individual organs and their locations. However, they would need to use more samples, particularly those presenting similar lesions. This could be very beneficial for the meat processing and veterinary medicine industries. Hyperspectral imaging technologies are non-invasive and non-contact, with the potential to enable automatic sorting of livestock organs and disease detection in the abattoir, allowing animal health reports to be provided for producers.

Acknowledgements

To Rapiscan Systems and Meat and Livestock Australia (MLA) Donor Company for their financial support towards the prototype multi-sensory platform (project P.PSH.0930) and for providing the first author Cassius Coombs' PhD Scholarship (B.STU.2018). Dr Michelle Henry of Gundagai Meat Processors is acknowledged for providing the healthy and diseased organs. The technical assistance of Dr Juan Molfino, Dr Milad Bagheri Shirvan, Dr Janine Chang Fung Martel, Schyla Butcher, and John Kelly from The University of Sydney, and Dr Russell Standish and Greig Turner from Rapiscan Systems is greatly appreciated. Dr Garth Tarr was supported by the Australian Research Council (DP210100521).

This project is supported by funding from the Australian Government Department of Agriculture, Water and the Environment as part of its Rural R&D for Profit programme in partnership with Research & Development Corporations, Commercial Companies, State Departments & Universities.

Conflict of Interest Statement

The funding bodies mentioned above had no influence on the experimental design or analysis of results.

References

AHDB. 2017. Abattoir post-mortem conditions guide (O. Doxon, Ed.). Agriculture and Horticulture Development Board: Kenilworth, UK. Available at: https://projectblue.blob.core.windows.net/media/Default/Imported%20Publication%20Docs/AHDB%20Beef%20and%20Lamb/AbattoirGuide_1555_180917_WEB.pdf. Accessed 20 September 2021.

Arsenault, J., Girard, C., Dubreuil, P., Daignault, D., Galarneau, J-R., Boisclair, J., Simard, C., and Bélanger, D. 2003. Prevalence of and carcass condemnation from maedi-visna, paratuberculosis and caseous lymphadenitis in culled sheep from Quebec, Canada. Prev. Vet. Med. 59: 67-81. doi:10.1016/S1067-5877(03)00060-6.

Baeten, V., Fernández Pierna, J.A., and Dardenne, P. 2007. Hyperspectral imaging techniques: an attractive solution for the analysis of biological and agricultural materials. In: H. F. Grahn, P. Geladi, eds., Techniques and applications of hyperspectral image analysis. John Wiley & Sons, Ltd., Chichester, UK, p. 289-211. doi:10.1002/9780470010884.ch12.

Butler, R. J., Murray, J. G., and Tidswell, S. 2003. Quality assurance and meat inspection in Australia. Rev. Sci. Tech. 22: 697-712. doi:10.20506/rst.22.2.1430.

This project is supported by funding from the Australian Government Department of Agriculture, Water and the Environment as part of its Rural R&D for Profit programme in partnership with Research & Development Corporations, Commercial Companies, State Departments & Universities.

Chen, Y-R., and Kim. M. S. 2004. Visible/NIR imaging spectroscopy for assessing quality and safety of agro-foods. Near Infr. Spectr. Int. Conf. Proc., Cordoba, Spain, p. 67-68. Available at: https://www.ars.usda.gov/research/publications/publication/?seqNo115=149531. Accessed 8 September 2021.

Cheng, J-H., and Sun, D-W. 2015. Rapid and non-invasive detection of fish microbial spoilage by visible and near infrared hyperspectral imaging and multivariate analysis. LWT – Food Sci. Tech. 62: 1060-1068. doi:10.1016/j.lwt.2015.01.021.

Coombs, C. E. O., Allman, B. E., Morton, E. J., Gimeno, M., Horadagoda, N., Tarr, G., and González, L. A. 2021. A preliminary investigation into the differentiation of sheep and cattle organs using visible and short-wave infrared hyperspectral imaging. Food Control, submitted.

Cutler, D. R., Edwards Jr, T. C., Beard, K. H., Cutler, A., Hess, K. T., Gibson, J., and Lawler, J. J. 2007. Random forests for classification in ecology. Ecology 88: 2783-2792. doi:10.1890/07-0539.1.

Elmasry, G., Barbin, D. F., Sun, D., and Allen, P. 2012a. Meat quality evaluation by hyperspectral imaging technique: An overview. Crit. Rev. Food Sci. Nutr. 52: 689-711. doi:10.1080/10408398.2010.507908.

Elmasry, G., Sun, D-W., and Allen, P. 2012b. Near-infrared hyperspectral imaging for predicting colour, pH and tenderness of fresh beef. J. Food Eng. 110:127-140. doi:10.1016/j.foodeng.2011.11.028.

Ezanno, P., Picault, S., Beaunée, G., Bailly, X., Muñoz, F., Duboz, R., Monod, H., and Guégan, J-F. 2021. Research perspectives on animal health in the era of artificial intelligence. BMC Vet. Res. 52: 40. doi:10.1186/s13567-021-00902-4.

This project is supported by funding from the Australian Government Department of Agriculture, Water and the Environment as part of its Rural R&D for Profit programme in partnership with Research & Development Corporations, Commercial Companies, State Departments & Universities.

GIMP Development Team (2020). *GNU Image Manipulation Program (Version 2.10.18)*. GIMP, University of California, Berkeley, CA. http://gimp.org/.

Goodwin-Ray, K. A., Stevenson, M. A., Heuer, C., and Cogger, N. 2008. Economic effect of pneumonia and pleurisy in lambs in New Zealand. N. Z. Vet. J. 56: 107-114. doi:10.1080/00480169.2008.36818.

Huang, H., Liu, L., and Ngadi, M. O. 2014. Recent developments in hyperspectral imaging for assessment of food quality and safety. Sensors 14: 7248-7276. doi:10.3390/s140407248.

Jones, G. E., Field, A. C., Gilmour, J. S., Rae, A. G., Nettleton, P. F., and McLauchlan, M. 1982. Effects of experimental chronic pneumonia on bodyweight, feed intake and carcase composition of lambs. Vet. Rec. 110: 168-173. doi:10.1136/vr.110.8.168.

Kamruzzaman, M., Haque, M. E., and Ali, M. R. 2014. Hyperspectral imaging technique for offal quantification in minced meat. J. Bangl. Agric. Uni. 12: 189-194. doi:10.3329/jbau.v12i1.21411.

Kong, W., Zhang, C., Liu, F., Nie, P., and He, Y. Rice seed cultivar identification using near-infrared hyperspectral imaging and multivariate data analysis. Sensors 13: 8916-8927. doi:10.3390/s130708916.

Kucheryavskiy, S. 2020. mdatools – R package for chemometrics. Chemometr. Intell. Lab. Syst. 98: 103937. doi:10.1016/j.chemolab.2020.103937.

Kucheryavskiy, S. 2021. Package 'mdatools' – multivariate data analysis for chemometrics. R package version 0.11.5. https://cran.r-project.org/web/packages/mdatools/mdatools.pdf. Accessed April 30, 2021.

Kuhn, M. 2008. Building predictive models in R using the caret package. J. Stat. Softw. 88: 5. doi:10.18637/jss.v028.i05.

This project is supported by funding from the Australian Government Department of Agriculture, Water and the Environment as part of its Rural R&D for Profit programme in partnership with Research & Development Corporations, Commercial Companies, State Departments & Universities.

Kuhn, M. 2021. Caret: Classification and regression training. R package version 6.0-86.

Lacasta, D. Ferrer, L. M., Ramos, J. J., González, J. M., and De las Heras, M. 2008. Influence of climatic factors on the development of pneumonia in lambs. Small. Rum. Res. 80: 28-32. doi:10.1016/j.smallrumres.2008.08.004.

Lawrence, R. L., Wood, S. D., and Sheley, R. L. 2006. Mapping invasive plants using hyperspectral imagery and Breiman Cutler classifications (randomForest). Remote Sens. Environ. 100: 356-362. doi:10.1016/j.rse.2005.10.014.

Lee, K. J., Kishimoto, M., Shimizu, J., Kobayashi, Y., Matsumoto, K., Sasaki, N., Ishii, M., Inokuma, H., Iwasaki, T., Miyake, Y., and Yamada, K. 2011. Use of contrast-enhanced CT in the diagnosis of abscesses in cattle. J. Vet. Med. Sci. 73: 113-115. doi:10.1292/jvms.10-0233.

Lee, K., Yamada, K., Tsuneda, R., Kishimoto, M., Shimizu, J., Kobayashi, Y., Furuoka, H., Matsui, T., Sasaki, N., Ishii, M., Inokuma, H., Miyake, Y., and Iwasaki, T. 2009. Clinical experience of using multidetector-row CT for the diagnosis of disorders in cattle. Vet. Rec. 165: 559-562. doi:10.1136/vr.165.19.559.

Liaw, A., and Wiener, M. R. 2002. Classification and regression by randomForest. R News 2: 18-22.

Mao, R., Qi, H., Pei, L., Hao, J., Dong, J., Jiang, T., Ainiwaer, A., Shang, G., Xu, L., Shou, X., Zhang, S., Wu, G., Lu, P., Bao, Y., and Li, H. 2017. CT scanning in identification of sheep cystic echinococcosis. BioMed. Res. Int. 2017, 4639202. doi:10.1155/2017/4639202.

McKinney, S. M., Sieniek, M., Godbole, V., Godwin, J., Antropova, N., Ashrafian, H., Back, T., Chesus, M., Corrado, G. C., Darzi, A., Etemadi, M., Garcia-Vicente, F., Gilbert, F. J., Halling-Brown, M., Hassabis, D., Jansen, S., Karthikesalingam, A., Kelly, C. J., King, D., Ledsam, J. R., Melnick, D., Mostofi, H., Peng, L., Reicher, J. J., Romera-Paredes, B.,

This project is supported by funding from the Australian Government Department of Agriculture, Water and the Environment as part of its Rural R&D for Profit programme in partnership with Research & Development Corporations, Commercial Companies, State Departments & Universities.

Sidebottom, R., Suleyman, M., Tse, D., Young, K. C., De Fauw, J., and Shetty, S. 2020. International evaluation of an AI system for breast cancer screening. Nature 577: 89-94. doi:10.1038/s41586-019-1799-6.

Murray, G. 1986. Ante-mortem and post-mortem meat inspection: an Australian Inspection Service perspective. Aust. Vet. J. 63: 211-215. doi:10.1111/j.1751-0813.1986.tb02997.x.

Nade, T., Fujita, K., Fujii, M., Yoshida, M., Haryu, T., Misumi, S., and Okumura, T. 2005. Development of x-ray computed tomography for live standing cattle. Anim. Sci. J. 76: 513-517. doi:10.1111/j.1740-0929.2005.00298.x.

Nakariyakul, S., and Casasent, D. P. 2009. Fast feature selection algorithm for poultry skin tumor detection in hyperspectral data. J. Food Eng. 94: 358-365. doi:10.1016/j.foodeng.2009.04.001.

Neethirajan, S., Tuteja, S. K., Huang, S-T., Kelton, D. 2017. Recent advancement in biosensors technology for animal and livestock health management. Biosens. Bioelectron. 98: 398-407. doi:10.1016/j.bios.2017.07.015.

R Core Team 2020. R: A language and environment for statistical computing. R Foundation for Statistical Computing, Vienna, Austria. www.R-project.org.

Samuel, J. L., O'Boyle, D. A., Mathers, W. J., & Frost, A. J. 1980. The contamination with Salmonella of bovine livers in an abattoir. Aust. Vet. J. 56: 526-528. doi:10.1111/j.1751-0813.1980.tb02579.x.

Scholz, A.M., Bünger, L., Kongsro, J., Baulain, U., and Mitchell, A.D. 2015. Non-invasive methods for the determination of body and carcass composition in livestock: dual energy X-ray absorptiometry, computed tomography, magnetic resonance imaging and ultrasound: a review. Animal 9: 1250-1264. doi:10.1017/S1751731115000336.

This project is supported by funding from the Australian Government Department of Agriculture, Water and the Environment as part of its Rural R&D for Profit programme in partnership with Research & Development Corporations, Commercial Companies, State Departments & Universities.

Thomas-Bachli, A. L., Pearl, D. L., Friendship, R. N., and Berke, O. 2014. Exploring relationships between whole carcass condemnation abattoir data, non-disease factors and disease outbreaks in swine herds in Ontario (2001-2007). BMC Res. Notes 7: 185. doi:10.1186/1756-0500-7-185.

Toohey, E. S., van de Ven, R., and Hopkins, D. L. 2018. The value of objective online measurement technology: Australian red meat processor perspective. Anim. Prod. Sci. 58: 1559-1565. doi:10.1071/AN17775.

Uzal, F. A., More, S. J., Dobrenov, B., and Kelly, W. R. 2002. Assessment of organoleptic post-mortem inspection techniques for bovine offal. Aust. Vet. J. 80: 70-74. doi:10.1111/j.1751-0813.2002.tb12841.x.

Webber, J. J., Dobrenov, B., Lloyd, J., and Jordan, D. 2012. Meat inspection in the Australian red meat industries: past, present and future. Aust. Vet. J. 90: 363-369. doi:10.1111/j.1751-0813.2012.00972.x.

Wickham, H., Averick, M., Bryan, J., Chang, W., D'Agostino McGowan, L., François, R., Grolemund, G., Hayes, A., Henry, L., Hester, J., Kuhn, M., Lin Pedersen, T., Miller, E., Milton Bache, S., Müller, K., Ooms, J., Robinson, D., Seidel, D. P., Spinu, V., Takahashi, K., Vaughan, D., Wilke, C., Woo, K., and Yutani, H. 2019. Welcome to the Tidyverse. J. Open Source Softw. 4: 1686. doi:10.21105/joss.01686.

Williams, P., Dardenne, P., and Flinn, P. 2017. Tutorial: Items to be included in a report on a near infrared spectroscopy project. J. Near Infrared Spectrosc. 25: 85-90. doi:10.1177/0967033517702395.

Wilson, C. S., Jenkins, D. J., Barnes, T. S., and Brookes, V. J. 2019. Evaluation of the diagnostic sensitivity and specificity of meat inspection for hepatic hydatid disease in beef cattle

This project is supported by funding from the Australian Government Department of Agriculture, Water and the Environment as part of its Rural R&D for Profit programme in partnership with Research & Development Corporations, Commercial Companies, State Departments & Universities.

in an Australian abattoir. Prev. Vet. Med. 167: 9-15. doi:10.1016/j.prevetmed.2019.03.014.

Wu, D., Sun, D-W., and He, Y. 2012. Application of long-wave near infrared hyperspectral imaging for measurement of color distribution in salmon fillet. Innov. Food Sci. Emerg. Technol. 16: 361-372. doi:10.1016/j.ifset.2012.08.003.

Xu, J-L., and Sun, D-W. 2017. Hyperspectral imaging technique for on-line monitoring of meat quality and safety. In: F. Toldrá and L. M. L. Nollet, eds., Advanced technologies for meat processing. CRC Press, Boca Raton, FL, p. 17-82. doi:10.1201/9781315152752-2.

This project is supported by funding from the Australian Government Department of Agriculture, Water and the Environment as part of its Rural R&D for Profit programme in partnership with Research & Development Corporations, Commercial Companies, State Departments & Universities.

Table 1. Gross interpretation of lesions found in sheep organs after slaughter.

Lesion	Heart	Kidney	Liver	Lung	Total
Granuloma	0	0	0	1	1
Fibrosis	0	0	1	1	2
Haemorrhage	1	1	1	1	6
Mineralisation	0	0	4	0	4
Pneumonia	n/a	n/a	n/a	5	5
Caseous lymphadenitis	0	0	1*	6**	7
Pyelonephritis	0	1	0	0	1
Atelectasis	0	0	0	1	1
Lobe reddening	0	0	0	1	1
Myocarditis	1	0	0	0	1
Hepatitis	0	0	1	0	1
Circumscribed lesion	0	0	1	0	1
Abscessation	0	0	0	2	2
Nodules in lobes	0	0	0	1	1
Ventricle lesion	1	0	0	0	1
Bronchiectasis	0	0	0	1	1
Discolouration but NDL***	10	4	2	0	16
Total Diseased	**13**	**6**	**11**	**17**	**47**
Total Healthy	**15**	**9**	**13**	**5**	**42**
Total	**28**	**15**	**24**	**22**	**89**

* Found in the hepatic lymph node. ** Found in the mediastinal lymph node. *** NDL – no detectable lesions.

This project is supported by funding from the Australian Government Department of Agriculture, Water and the Environment as part of its Rural R&D for Profit programme in partnership with Research & Development Corporations, Commercial Companies, State Departments & Universities.

Table 2. Goodness-of-fit statistics from hyperspectral (HS) data used to differentiate between diseased or healthy organs of sheep from commercial slaughter.

Spectral range	Statistic						
	Method	Tuning	Accuracy	Kappa	Sensitivity	Specificity	Precision
				Heart			
VIS	PLS-DA	5	0.85	0.70	0.75	0.93	0.90
	RF	430	0.78	0.54	0.67	0.87	0.80
SWIR	PLS-DA	7	0.89	0.79	0.92	0.87	0.86
	RF	480	0.82	0.64	0.77	0.87	0.83
COMB	PLS-DA	5	0.85	0.70	0.83	0.87	0.83
	RF	300	0.85	0.70	0.83	0.87	0.83
				Kidney			
VIS	PLS-DA	7	0.73	0.44	0.67	0.78	0.67
	RF	470	0.60	0.17	0.50	0.67	0.50
SWIR	PLS-DA	6	0.87	0.71	0.67	1.00	1.00
	RF	320	0.73	0.41	0.50	0.89	0.75
COMB	PLS-DA	1	0.80	0.57	0.67	0.89	0.80
	RF	470	0.73	0.41	0.50	0.89	0.75
				Liver			
VIS	PLS-DA	4	0.88	0.75	0.82	0.92	0.90
	RF	450	0.83	0.66	0.73	0.92	0.89
SWIR	PLS-DA	2	0.92	0.83	0.91	0.92	0.91
	RF	410	0.92	0.83	0.91	0.92	0.91
COMB	PLS-DA	4	0.96	0.92	0.91	1.00	1.00
	RF	390	0.88	0.75	0.82	0.92	0.90
				Lung			
VIS	PLS-DA	1	0.67	-0.16	0.88	0.00	0.74
	RF	330	0.76	0.17	0.93	0.20	0.79
SWIR	PLS-DA	6	0.91	0.70	1.00	0.60	0.90
	RF	430	0.73	-0.08	0.94	0.00	0.76
COMB	PLS-DA	2	0.81	0.39	0.94	0.40	0.83
	RF	380	0.76	0.17	0.94	0.20	0.79

VIS visible; SWIR – short-wave infrared; COMB – combination VIS and SWIR; PLS-DA – partial least squares discriminant analysis; RF -random forest; Tuning – number of components (*ncomp*) for PLS-DA and number of nodes available for each tree splitting (*mtry*) for RF

This project is supported by funding from the Australian Government Department of Agriculture, Water and the Environment as part of its Rural R&D for Profit programme in partnership with Research & Development Corporations, Commercial Companies, State Departments & Universities.

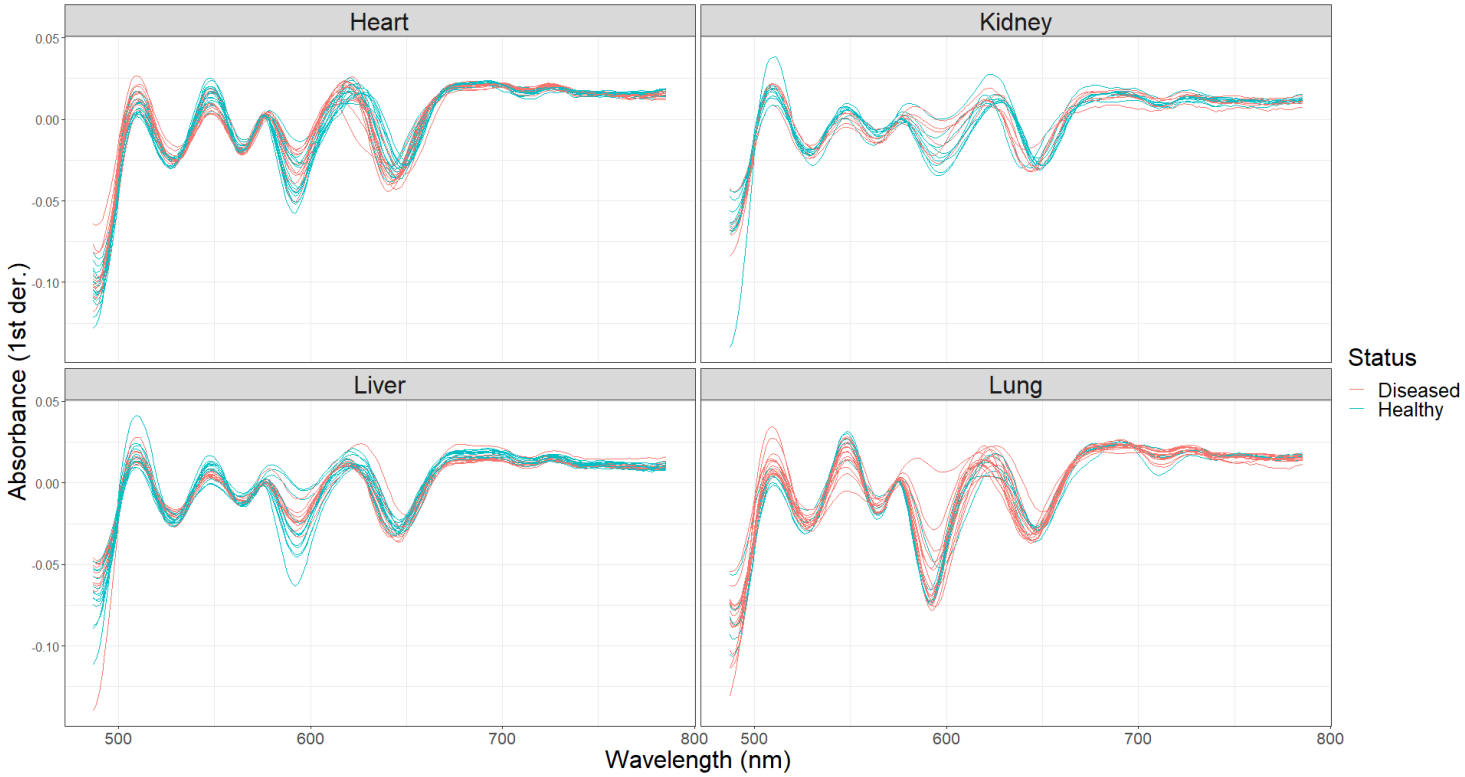

Fig. 1. Transformed (first derivative) and smoothed (centred moving average) visible absorbance hyperspectral data of healthy and diseased sheep organs.

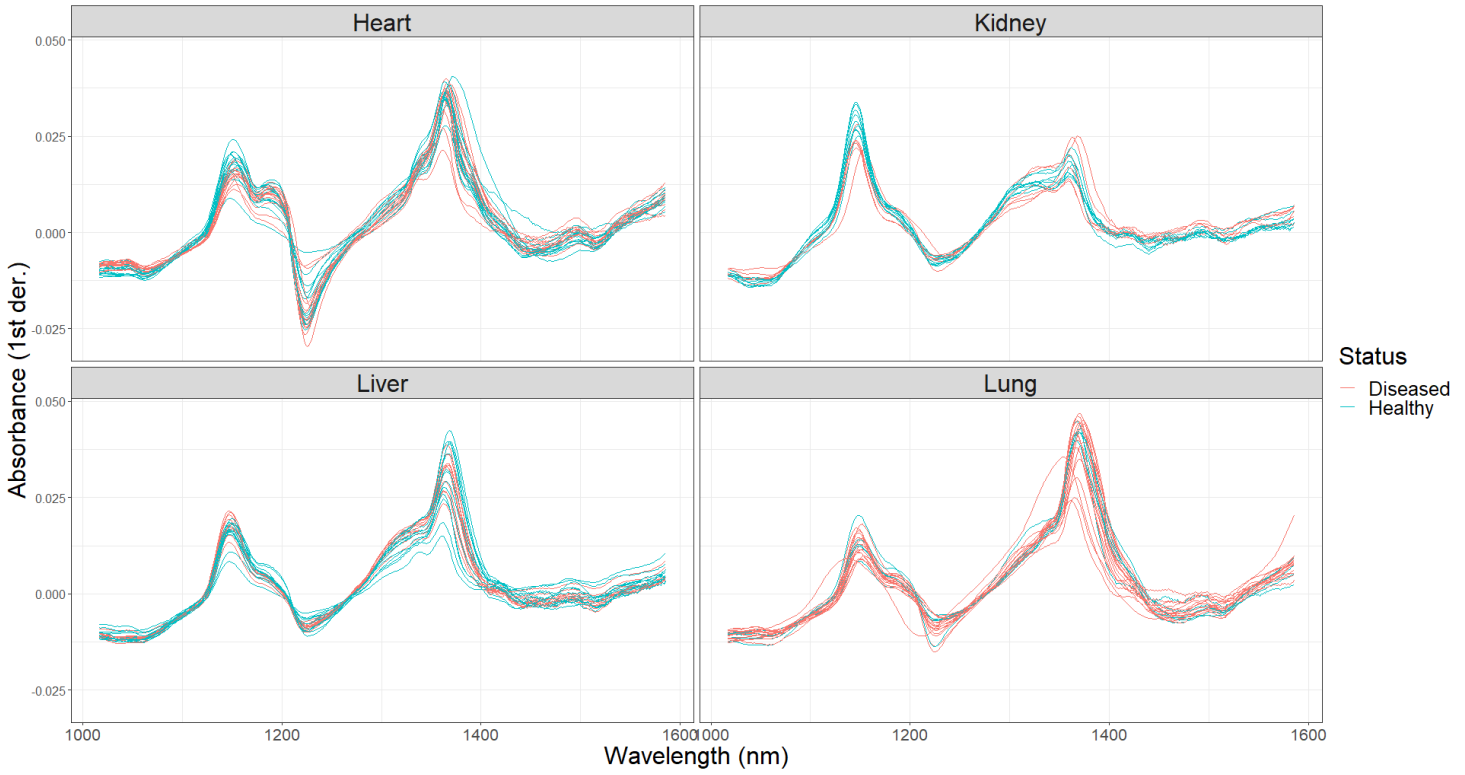

This project is supported by funding from the Australian Government Department of Agriculture, Water and the Environment as part of its Rural R&D for Profit programme in partnership with Research & Development Corporations, Commercial Companies, State Departments & Universities.

Fig. 2. Transformed (first derivative) and smoothed (centred moving average) short-wave infrared absorbance hyperspectral data of healthy and diseased sheep organs.

Appendix. Examples of images from normal camera (RGB), hyperspectral (HS) and MEXA (X-ray) of sheep organs with defects used to automatic detection using Rapiscan MEXA scanner.

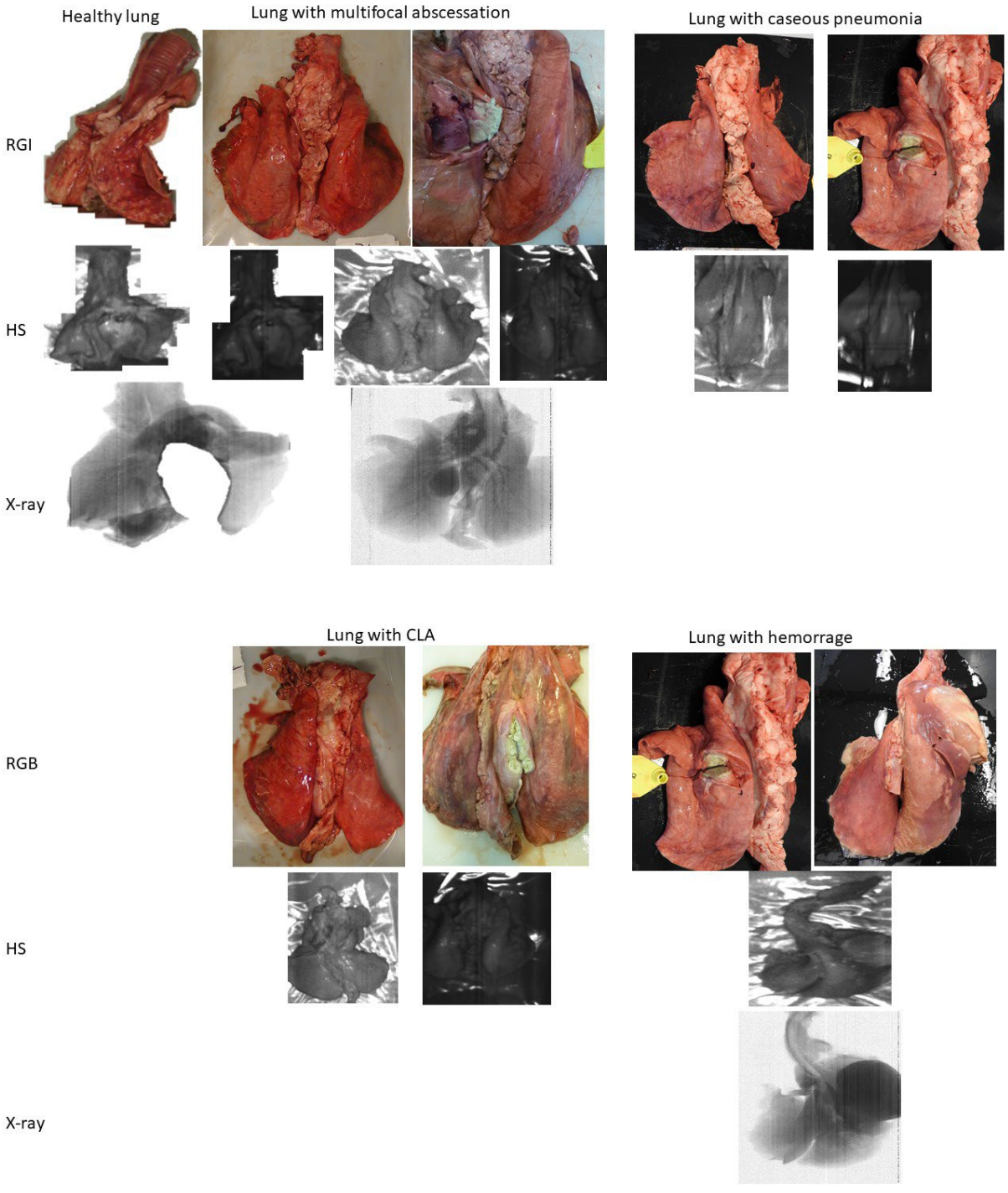

This project is supported by funding from the Australian Government Department of Agriculture, Water and the Environment as part of its Rural R&D for Profit programme in partnership with Research & Development Corporations, Commercial Companies, State Departments & Universities.

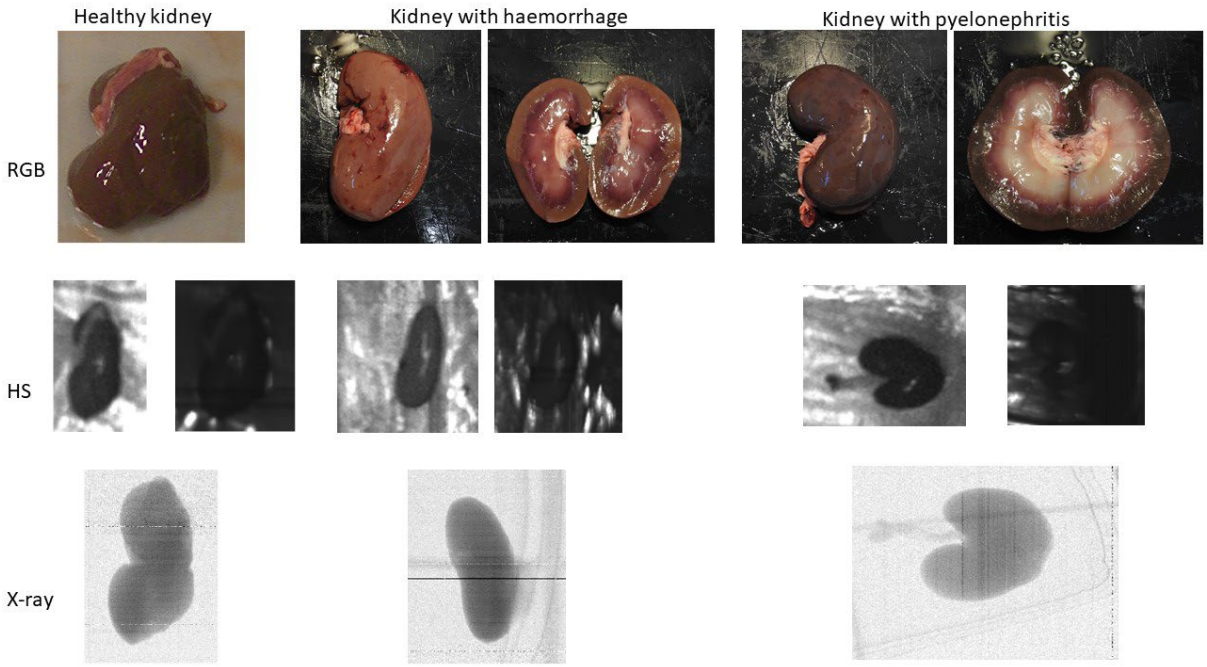

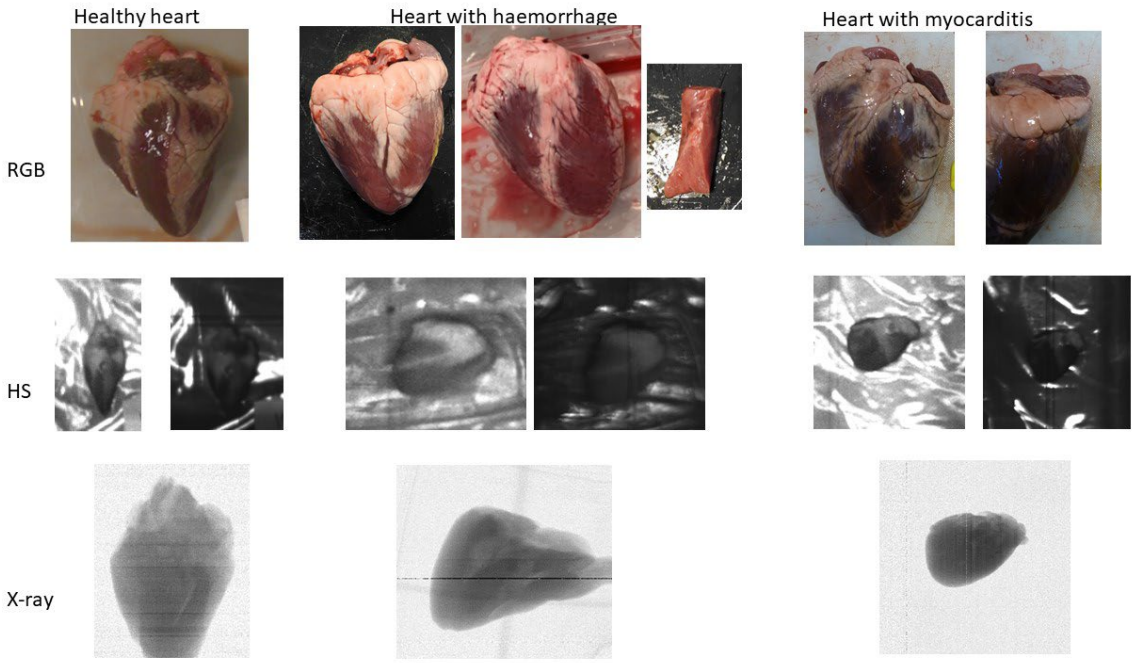

This project is supported by funding from the Australian Government Department of Agriculture, Water and the Environment as part of its Rural R&D for Profit programme in partnership with Research & Development Corporations, Commercial Companies, State Departments & Universities.

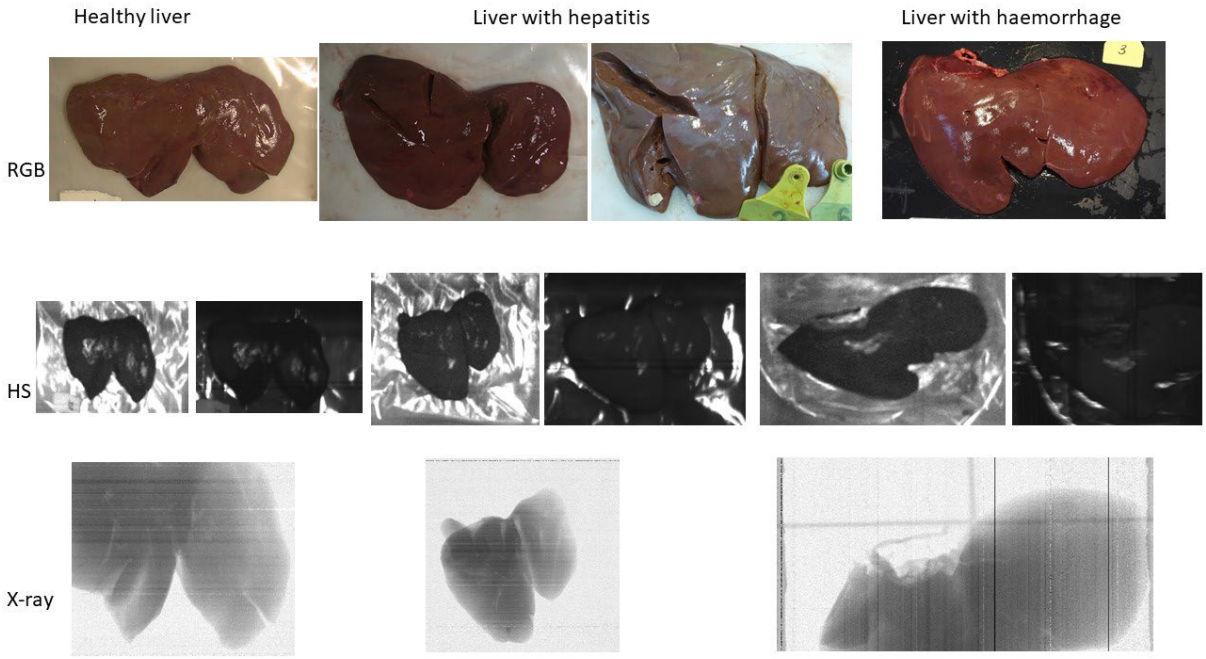

This project is supported by funding from the Australian Government Department of Agriculture, Water and the Environment as part of its Rural R&D for Profit programme in partnership with Research & Development Corporations, Commercial Companies, State Departments & Universities.

5 Conclusion

The V.RDP.2018 program has demonstrated that the combination of dual-view multi-energy X-ray analysis, visible wavelength hyperspectral imaging and short wave infra-red hyperspectral imaging has the potential to deliver accurate identification of different tissue types and disease in real-time in an abattoir setting.

Considerably more work will be required to collect larger reliable, curated, data sets upon which to evaluate and further develop in-depth, accurate, algorithms to deliver automated inspection results at abattoir throughput rates. However, the collaborative development program established through the V.RDP.2016 and V.RDP2018 programs is starting to show promise for MEXA assisted automated offal sortation.

To support the on-going data collection exercise and to drive the application of automated health screening in abattoirs and packaged meat processing plants, MLA, Rapiscan and the University plan to establish a steering committee including the Gundagai abattoir and other meat processors to focus the next phase of this work now that the core scanning technology is in place and initial results look to be promising.

This project is supported by funding from the Australian Government Department of Agriculture, Water and the Environment as part of its Rural R&D for Profit programme in partnership with Research & Development Corporations, Commercial Companies, State Departments & Universities.